EMERGENCE OF A-SITE CATION ORDER IN THE SMALL RARE-EARTH MELILITES $SrREGa_3O_7$ (RE = Dy–Lu, Y)

Haytem Bazzaoui[a], Cécile Genevois[a], Marina Boyer[a], Sandra Orya, Yannick Ledemi[b], Younès Messaddeq[b], Michael Pitcher[a], and Mathieu Allix[a]

[a] *CNRS, CEMHTI UPR 3079, Univ. Orléans, F-45071 Orléans, France.*
[b] *Univ Laval, Dept Phys Engn Phys & Opt, Ctr Opt Photon & Lasers, Pav Opt Photon, 2375 Rue Terrasse, Quebec City, PQ G1V 0A6, Canada.*
mathieu.allix@cnrs-orleans.fr

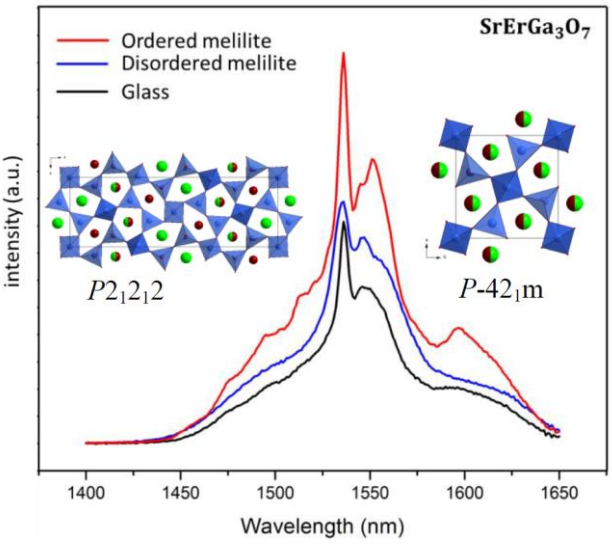

Figure 1. Photoluminescence emission spectra recorded on $SrErGa_3O_7$ Glass in black, Disordered polymorph in blue and the Ordered 3x1x1 melilite in red.

The ABC_3O_7 melilite structure type is a well-known host matrix for luminescent materials [1-2]. It crystallizes in a tetragonal system within a P-42$_1$m space group and cell parameters of a≈7.93 Å, c≈5.22 Å, according to a layered structure along the z axis formed by corner-sharing MO_4 tetrahedra, between which alkaline earth and/or rare earths cations are located [3]. This structure type allows certain flexibility on the cations size that can be inserted between the layers. Using an alternative synthesis process "full and congruent crystallization from glass", facilitated by a unique melt-quenching approach (aerodynamic levitation coupled to a CO_2 laser), a new $SrREGa_3O_7$ melilite superstructure, which is a 3-fold (3a x b x c) superstructure of the melilite sub-cell, crystallizes for small rare earths (RE = Dy – Lu, Y). Depending on the proceeded heat treatment on glass samples both disordered and ordered melilites can be stabilized independently, as transparent bulk ceramics. This new superstructure crystallizes in an orthorhombic system within a $P2_12_12$ space group and cell parameters of a≈23.79Å, b≈7.93Å and c≈5.22 Å, with the same layered sub-structure. This superstructure is due to an ordering of the A site cations among the a axis which results in a 3-fold expansion of the a parameter. The photoluminescence emission spectra show a clear restructuration of the bands and a maximum intensity that is almost doubled in comparison with the glass and the disordered polymorph emission bands This is related to the introduction of a completely dedicated site for the rare earth in addition to the mixed Sr/RE site, compared to the disordered polymorph which contains only one mixed A-cation site. Optimization of the luminescence properties can be induced by a structural ordering which we have shown here by comparing the ordered and disordered melilite photoluminescence emission spectra.

[1] A. A. Kaminskii, H. H. Yu, J. Y. Wang, Y. Y. Zhang, H. J. Zhang, O. Lux, H. Rhee, H. J. Eichler, J. Hanuza, H. Yoneda and A. Shirakawa, *Laser Phys*., 2014, **24**, 085803.
[2] M. Karbowiak, P. Gnutek, C. Rudowicz and W. Ryba-Romanowski, *Chem. Phys.*, 2011, **387**, 69–78.
[3] M. Boyer, A. J.F. Carrion, S. Ory, A. I. Becerro, S. Villette, S. V. Eliseeva, S. Petoud, P. Aballea, G. Matzen, M. Allix, *J. Mater. Chem. C*, 2016, **4**, 3238–3247.

COLLOIDAL SYNTHESIS OF RARE EARTH-BASED SEMICONDUCTING NANOCRYSTALS FOR THE SENSITIZATION OF RARE EARTH PHOTOLUMINESCENCE

Guillaume Gouget,[†] Morgane Pellerin,[‡] Rabih Al Rahal Al Orabi,[▽] Lauriane Pautrot-D'Alençon,[‡] Thierry Le Mercier,[‡] and Christopher B. Murray[*,†]

[†]*Department of Chemistry, University of Pennsylvania, Philadelphia, Pennsylvania 19104, United States*
[‡]*Solvay, Research and Innovation Center Paris, F-93308, Aubervilliers, France*
[▽]*Solvay, Design and Development of Functional Materials Department, Axel'One, 87 avenue des Frères Perret, 69192 Saint Fons, Cedex, France*

Nanocrystals (NCs) with luminescent rare earth (RE) ions are attractive for their potential applications in several fields such as bio-imaging, light-emitting displays, anti-counterfeiting technologies, telecommunication, lasing, and high-energy photon detection. The narrow absorption cross-section of RE ions is a major drawback for their photoluminescence (PL) efficiency. Semiconducting NCs as RE hosts are attracting for broadband sensitization of RE PL in the visible range,[1–4] with tunable absorption range depending on size and shape of NCs in the quantum-confined regime.

RE chalcogenides would be ideal host nanostructures, with high insertion rates of RE emitters and bandgap energies between 1.6 and 2.9 eV in the sulfides of the lanthanide series. Bulk RE sulfides are diverse by means of composition, with RE +2 and/or +3 valences and S -2 and/or -1 valences stabilized among the various structures. However, europium monosulfide is the only representative stabilized as colloidal dispersions of NCs to date. New synthetic routes to RE chalcogenides NCs with controlled compositions, sizes and shapes are necessary to develop technologies based on photoluminescent RE ions sensitized by semiconducting NCs.

We present an original synthesis of colloidal RE sulfide NCs, based on the reaction of RE iodides and elemental sulfur or (bis-trimethylsilyl)sulfide ($(TMS)_2S$) in oleylamine. Mono-, sesqui- and disulfide NCs are isolated, as demonstrated with EuS, La_2S_3 and LaS_2. Phase speciation at the nanoscale between γ-La_2S_3 and LaS_2 relies on the choice of sulfur source. LaS_2 nanoellipsoids and nanoplates are obtained with thickness down to 2.8 nm. Size- and shape-dependent light absorption are characterized for EuS, La_2S_3 and LaS_2. We observe that Er^{3+} PL at 663 nm is excited in 10 % Er-doped La_2S_3 NCs *via* absorption of La_2S_3 semiconducting host from 390 to 450 nm.

These results should attract interest for applications relying on sensitized RE PL and motivate future works to stabilize diversified compositions and morphologies of RE chalcogenides as colloidal NCs.

References:

(1) Bol, A. A.; van Beek, R.; Meijerink, A. On the Incorporation of Trivalent Rare Earth Ions in II−VI Semiconductor Nanocrystals. *Chem. Mater.* **2002**, *14*, 1121–1126.

(2) Chengelis, D. A.; Yingling, A. M.; Badger, P. D.; Shade, C. M.; Pétoud, S. Incorporating Lanthanide Cations with Cadmium Selenide Nanocrystals: A Strategy to Sensitize and Protect Tb(III). *J. Am. Chem. Soc.* **2005**, *127*, 16752–16753.

(3) Martín-Rodríguez, R.; Geitenbeek, R.; Meijerink, A. Incorporation and Luminescence of Yb^{3+} in CdSe Nanocrystals. *J. Am. Chem. Soc.* **2013**, *135*, 13668–13671.

(4) Creutz, S. E.; Fainblat, R.; Kim, Y.; De Siena, M. C.; Gamelin, D. R. A Selective Cation Exchange Strategy for the Synthesis of Colloidal Yb^{3+}-Doped Chalcogenide Nanocrystals with Strong Broadband Visible Absorption and Long-Lived Near-Infrared Emission. *J. Am. Chem. Soc.* **2017**, *139*, 11814–11824.

DEVELOPMENT OF A TRICHROMATIC PHOSPHOR WITH TUNABLE EMISSION COLOR THROUGH A MACHINE LEARNING APPROACH

Estelle GLAIS[1], Florian MASSUYEAU[1], and Romain GAUTIER[1]

[1]*Université de Nantes, CNRS, Institut des Matériaux Jean Rouxel (IMN), F-44000 Nantes, France.*
estelle.glais@cnrs-imn.fr, https://www.cnrs-imn.fr/

Keywords: Luminescent material, dopant valence state, CIE diagram, Machine Learning

Summary: The discovery of new materials with optimized luminescence properties requires a huge number of assays. Fundamental understanding or predictive theories are not sufficient nor accurate enough to identify a material with specific properties. In this study, we focused on $Ca_{14}Zn_6Ga_{10}O_{35}$:Mn^{4+},Mn^{2+},Tm^{3+} (CZGO) phosphor. The three dopants exhibit luminescence properties in distinct spectral regions, namely red (Mn^{4+}), green (Mn^{2+}), and blue (Tm^{3+}) (see figure 1a). CZGO samples are synthesized in air according to a conventional solid state method, followed by a thermal treatment in reductive atmosphere. Five parameters that are able to influence the photoluminescence properties are identified. The resulting emission color can be tuned thanks to the temperature and the duration of the reductive thermal treatment, the concentration of Mn and Tm precursors as well as the excitation wavelength. Thus, the optimization of the luminescence properties of such single-phase material co-doped with three different activators remains challenging. In addition, charge transfers can occur between dopant ions, and consequently the control of each emitting center contribution is limited. To this end, we propose to combine experimental synthesis with a machine learning approach, in order to accelerate luminescence properties optimization. The resulting emission color of one single material can screen a broad range of emission colors (figure 1b), and the signature of the phosphor can be finely predicted, which can be very useful for many applications as LEDs, UV detection or anticounterfeiting.

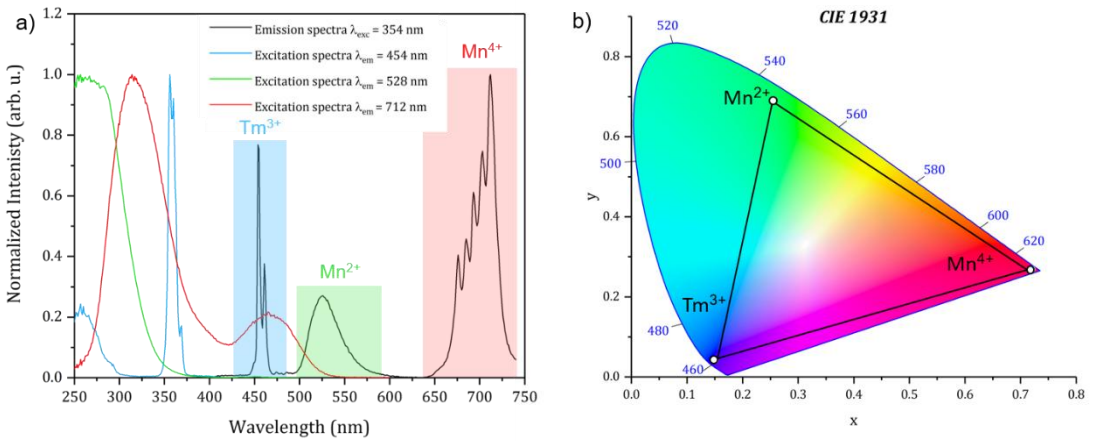

Fig. 1 a) Excitation and emission spectra of CZGO:Mn^{4+},Mn^{2+},Tm^{3+} phosphor b) CIE diagram of CZGO:Mn^{4+}, CZGO:Mn^{2+}, CZGO:Tm^{3+} phosphors (the dark line define the color range that can be reached by the studied phosphor).

MOLYBDENUM OCTAHEDRAL IODIDES: A NEW CLASS OF AMBIPOLAR MATERIALS FOR SOLAR ENERGY CONVERSION

Adèle Renaud,[1] Pierre-Yves Jouan,[2] Noée Dumait,[1] Nicolas Barreau,[2] Tetsuo Uchikochi,[3,4] Fabien Grasset,[1,3] Stéphane Jobic[2] and Stéphane Cordier[1]

[1]*Univ Rennes, CNRS, ISCR – UMR 6226, F-35000 Rennes, France*
[2]*Université de Nantes, CNRS, Institut des Matériaux Jean Rouxel, IMN, F-44000, Nantes, France*
[3]*CNRS–Saint-Gobain–NIMS, IRL 3629, Laboratory for Innovative Key Materials and Structures (LINK), National Institute for Materials Science, 1-1 Namiki, 305-0044 Tsukuba, Japan*
[4]*Research Center for Functional Materials, National Institute for Materials Science (NIMS), 1-1 Namiki, Tsukuba, Japan*
adele.renaud@univ-rennes1.fr, https://iscr.univ-rennes1.fr/adele-renaud

Keywords: Molybdenum octahedral cluster; ambipolar material; photoelectrochemistry; solar cell; electronic structure

Summary: Ambipolar materials are a class of compounds that can intrinsically transport and transfer simultaneously both charge carriers, holes and electrons in a comparable way.[1,2] Unlike conventional unipolar semiconductors in which a type of charge carrier is predominant, ambipolar materials can display p-type and n-type characteristics within a single device, which makes them attractive materials for many different application fields such as sunlight conversion.[2,3] Only few materials such as semiconducting polymers, carbon nanotubes, 2D materials or organic-inorganic hybrid perovskites exhibit ambipolar behaviors.[1-3] Their intriguing intrinsic electronic properties result from their specific electronic structures widely tuned by their morphology, composition and size.[1-3]
The authors recently investigated the ambipolar character of Mo_6 clusters compounds. Transition metal cluster (MC)-based halides are nano-objects that have a tri-dimensional size restriction giving them fascinating optical and electronic properties such as molecule-like energy gaps, strong absorption in the visible and/or NIR spectral regions, deep red luminescence or high (photo)catalytic properties.[4-6] Outstanding ambipolar properties of MC compounds were highlighted through a range of photoelectrochemical characterizations and led to the design, as a demonstrator, of an all solid solar cell integrating a MC-based light-harvester.[7] Thus, this presentation will be focused on the evidence of the ambipolar character of Mo_6 cluster iodides, from its origin to its interest for solar energy conversion.

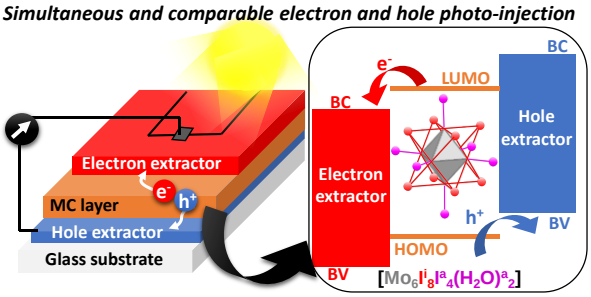

Fig. 1 All solid solar cell structure prepared from ambipolar MC iodide.

References:
1. Ren, Y.; Han, S.-T.; Zhou, Y., *Smart Materials Series*, RSC **2021**, 1-13.
2. Bisri, S. Z. ; Piliego, C. ; Gao, J.; Loi, M. A., *Adv. Mater.* **2014**, *26*, 1176-1199.
3. Giorgi, G.; Yamashita, K., *J. Mater. Chem. A* **2015**, *3*, 8981-8991.
4. Renaud, A.; Nguyen, T. K. N.; Grasset, F.; Raissi, M.; Guillon, V.; Delabrouille, F.; Dumait, N.; Jouan, P.-Y.; Cario, L.; Jobic, S.; Odobel, F.; Cordier, S.; Uchikoshi, T., *Electrochimica Acta* **2019**, *317*, 737-745.
5. Zhao Y.; Lunt, R. R., *Adv. Energy Mater* **2013**, *3*, 1143-1148.
6. Feliz, M.; Puche, M.; Atienzar, P.; Concepción, P.; Cordier, S.; Molard, Y.; *ChemSusChem* **2016**, 9, 1963-1971.
7. Renaud, A.; Jouan, P.-Y. Dumait, N.; Barreau, N.; Uchikochi, T.; Grasset, F.; Jobic, S.; Cordier, S.; *ACS Appl. Mater. Interfaces*, Submitted

Eu^{3+}/Tb^{3+} MIXED METAL-ORGANIC FRAMEWORKS (MOFS) FOR RATIOMETRIC LUMINESCENT THERMOMETRY

Thibault Amiaud,* Rémi Dessapt* and Hélène Serier-Brault*

** Institut des Matériaux Jean Rouxel (IMN), Université de Nantes, UMR CNRS 6502*
2 rue de la Houssinière, BP 32229, 44322 Nantes cedex 3, France
thibault.amiaud@cnrs-imn.fr

In 2012, Cui *et al.* have shown that **lanthanide mixed-MOFs** bearing two Ln^{3+} emitters (*i.e.* Tb^{3+} and Eu^{3+}) present a great potential for application as **ratiometric luminescent thermometers**.[1] Since then, numerous lanthanide-based MOFs have emerged as new luminescent thermometers due to the infinite possibilities offered by the incredible numbers of suitable organic ligands. However, no study focuses on the rationalization of the key parameters that control the thermometer performances such as **temperature sensing range** or **relative thermal sensitivity**.
In a previous work, the impact of the lanthanides composition on the thermometric properties has been studied by our group on a series of mixed Eu-Tb isophthalate MOF.[2] We evidenced that an increase of the Eu^{3+} molar content leads to an improvement of the relative thermal sensitivity with a concomitant decrease of the corresponding temperature sensing range.
In this study, we are focused on two series of isostructural mixed-MOFs built on the ligand 1,2,4,5-benzenetetracarboxylic acid (H_4Btec, Figure 1a), with general formula $[Tb_{1-x}Eu_x(HBtec)]_n$ and $[Gd_{0.5}Tb_{0.5-x}Eu_x(HBtec)]_n$ (Figure 1b). Here, we highlight for the first time the influence of Gd^{3+} addition on Tb^{3+}-to-Eu^{3+} energy transfer processes and thermometric properties. Indeed, the Gd^{3+} dilution decreases the Tb^{3+}-to-Eu^{3+} energy transfer efficiency and allowed the addition of Eu^{3+} in wider range without totally quench the emission of Tb^{3+}. Moreover, for compositions from 1 to 40% of Eu^{3+}, the relative thermal sensitivity has been increased by a factor of 3 and a shift of the corresponding temperature sensing range has been observed from 120 to 170 K (Figure 1c). This confirms the possibility to chemically modulate the thermometric properties. Theoretical calculations are in progress to determine the Ln^{3+} energy levels involved in the temperature-sensing process (Pr. Luis Carlos, Aveiro).

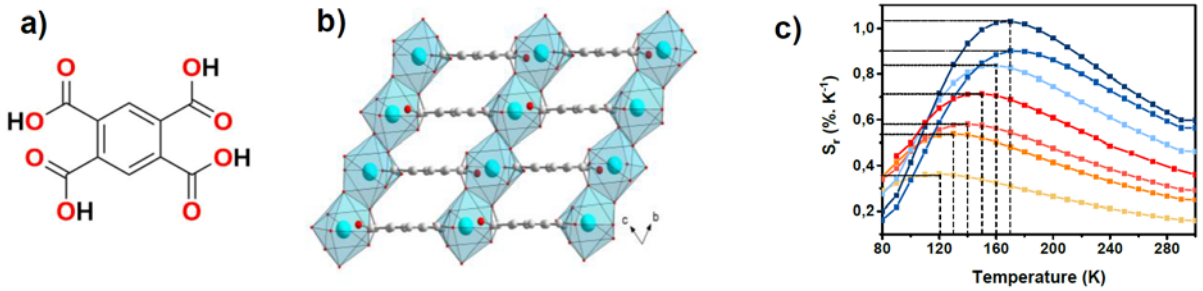

Figure 1. a) 1,2,4,5-benzenetetracarboxylic acid (H_4Btec). b) Crystal structure of $[Ln(HBtec)]_n$. c) Thermal evolution of the relative sensitivity in the $Tb_{1-x}Eu_x$ and $Gd_{0.5}Tb_{0.5-x}Eu_x$ series, in the 80-300 K range.

References

[1] Cui, Y; Xu, H; Yue, Y; Guo, Z; Yu, J; Chen, Z; Gao, J; Yang, Y; Qian, G and Chen, B, *J. Am. Chem. Soc.* **2012**, *134, 9,* 3979-3982.
[2] Trannoy, V; N. Carneiro Neto, A; D. S. Brites, C; D. Carlos, L; Serier-Brault, H, *Adv. Opt. Mater.* **2021,** 2001938

PLASMA DEPOSITED W/SiCH NANOCOMPOSITE AS HIGH TEMPERATURE AIR-STABLE SOLAR SELECTIVE ABSORBER COATINGS FOR CONCENTRATED SOLAR POWER RECEIVERS

Aïssatou DIOP[1], Danielle NGOUE[1,2], Amine MAHAMMOU[1,2], Babacar Diallo[3], Alex CARLING-PLAZA[1], Hervé GLENAT[1], Sébastien QUOIZOLA[1,2] Angélique BOUSQUET[4], Antoine GOULLET[5], Thierry SAUVAGE[3], Audrey SOUM-GLAUDE[1], Eric TOMASELLA[4], Laurent THOMAS[1,2]

[1]PROMES-CNRS (Laboratory of PROcess, Materials, Solar Energy)-Perpignan/Font-Romeu- Odeillo-Via, France
[2]Université de Perpignan, Perpignan, France
[3]CEMHTI (Conditions Extrêmes et Matériaux), Orléans, France
[4]ICCF (Institut de Chimie de Clermont-Ferrand), Aubière, France
[5]IMN (Institut des Matériaux Jean Rouxel), Nantes, France
aissatou.diop@promes.cnrs.fr, nanoplast-project.cnrs.fr

Keywords: CSP; Nanocomposites; Multilayers; Selective coating

Summary: Improving the performance of concentrated solar power technologies (CSP) requires the development of optically efficient innovative materials. One objective is to develop, by plasma deposition techniques, composite coatings with spectral selectivity, that is to say high absorption in the solar spectrum range (UV, visible and near infrared) and low emissivity in the infrared range to limit radiative thermal losses. These materials should also have other characteristics: resistance to high temperatures in air under concentrated solar conditions, and high resistance to the high amplitude cyclic thermomechanical stresses inherent to such applications.
High-performance solutions have been developed in PROMES laboratory such as, on one hand, dielectric-metal multilayer interference stacks, and on the other hand, ceramic-metal composites (cermets). Compared to multilayers, nanocomposites are known to be more resistant to oxidation, corrosion and thermomechanical stress. Indeed, their microstructure limits the diffusion of ambient oxygen into the coating by eliminating grain boundaries and improving mechanical properties (blocking of cracks propagation, resistance to deformation, etc.). As a matter of fact, previous optical simulations showed that cermet composites present higher heliothermal efficiencies compared to classical multilayers.
Composites were thus produced using two different plasma ways. The first one is by annealing multilayers to provoke interlayer diffusion. The latter are stacks associating a refractory metal (W) deposited by RF magnetron PVD and a ceramic (SiC:H) deposited by µwave-PACVD, allowing to improve solar absorptance (~ 89%) as well as thermal stability. The second way is by direct deposition of a SiC:H matrix with inclusions of W, by reactive magnetron sputtering, with or without assistance of ECR microwave sources. To highlight the high performance of these two types of materials, plasma process diagnostics (OES, laser diffusion) were coupled with material characterizations (SEM, EDS, XPS, RBS, Ellipsometry, UV-Vis-IR Reflectometry) of the monolayers and their association in high-performance stacks.
On one hand, for multilayers, coupling of SEM/EDS, RBS profiles and reflectometry measurements on annealed multilayers (500°C in air during 96 h) show W diffusion at W/SiC:H interfaces and Silicon oxidation at the top surface of the stacks (O~16%at.)(Fig. 1). Formation of a self-protective silicon based oxide top layer, with a low refractive index, and creation of complex SiC:H-W interlayers could explain the observed improvement of solar performance of the multilayers after thermal treatment in air. On the other hand, multimode AFM show that assisting reactive magnetron sputtering with microwave ECR excitation give rise to composites where W metal nanoparticules are homogeneously embedded in SiC:H matrix. (Fig. 2)
Those nanocomposites are proposed to be stacked in multilayers. Those two solutions present thermomechanical compatibilities with CSP applications.

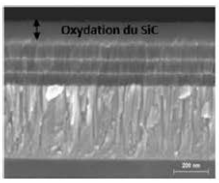

Fig. 1 MEB image of multilayers W/SiCH

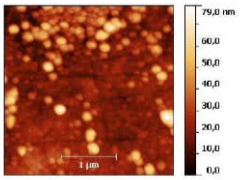

Fig. 2 AFM image of W-SiCH nanocomposite

SOLID-STATE SYNTHESIS OF BISMUTH PHOSPHATE HETEROJUNCTIONS WITH ENHANCED UV LIGHT EFFICIENCY IN PHOTOCATALYTIC DEGRADATION OF POLLUTANTS

Abdessalam BOUDDOUCH,[1] Elhassan AMATERZ,[2] Bahcine BAKIZ,[3] Aziz TAOUFYQ,[3] Frédéric GUINNETON,[4] Sylvie VILLAIN,[4] Jean-Raymond GAVARRI,[4] and Abdeljalil BENLHACHEMI[3]

[1] *Laboratoire de Réactivité et de Chimie des Solides, CNRS-UMR 7314, Université de Picardie Jules Verne, CEDEX 1, F-80039 Amiens, France.*

[2] Conditions Extrêmes et Matériaux : Haute Température et Irradiation CEMHTI - UPR3079 CNRS, Site Haute Température, Orléans, France

[3] *Laboratoire Matériaux et Environnement (LME), Faculté des Sciences, université Ibn Zohr, B.P 8106, Cite Dakhla, Agadir, Maroc.*

[4] *Institut Matériaux Microélectronique et Nanosciences de Provence, Université de Toulon, Aix Marseille Univ, CNRS, IM2NP, Toulon, France.*

abdessalam.bouddouch@u-picardie.fr , https://www.lrcs.u-picardie.fr

Keywords: $BiPO_4$ heterojunction; Solid-state; Photocatalytic activity; UV light; Rhodamine B; Methyl parathion.

Summary: The constructing of phase heterojunction photocatalytic system has received much attention in environmental purification and hydrogen generation from water [1]. In this study, a monoclinic bismuth phosphate heterojunctions were synthesized via a solid-state process [2]. The photocatalytic performance was evaluated by the degradation of rhodamine B (RhB) and Methyl parathion (MP) under UV-visible light irradiation. Results show that the as-synthesized $BiPO_4$ heterojunctions can significantly enhance photocatalytic activity in comparison with that of commercial particles of TiO_2, ZnO and Bi_2O_3.

The submicronic bismuth phosphate particles presented the highest apparent rate constant compared to those of the commercial materials in which the presence of surface defects could be behind this. These defects might be in relation with the specific photoluminescence observed under UV excitation [3, 4].

The detailed photocatalytic oxidative process of RhB under these different conditions was revealed by measurement of the UV-VIS spectra, HPLC, LC-MS and TOC analysis. A photocatalytic degradation mechanism of rhodamine B in the presence of $BiPO_4$ photocatalyst is proposed. The mineralization of rhodamine B is confirmed from total organic carbon (TOC).

References:

1. Hong, Y., Jiang, Y., Li, C., Fan, W., Yan, X., Yan, M., & Shi, W. *Applied Catalysis B: Environmental*, **2016**, 180, 663-673.
2. Bouddouch, A., Amaterz, E., Bakiz, B., Taoufyq, A., Guinneton, F., Villain, S., Gavarri, J-R., Valmalette, J-C. and Benlhachemi, A. *Minerals*, **2021**, *11*(9), 1007.
3. Bouddouch, A., Amaterz, E., Bakiz, B., Taoufyq, A., Guinneton, F., Villain, S., Gavarri, J-R., Valmalette, J-C. and Benlhachemi, A. *Water environment research*, **2020**, *92*(11), 1874-1887.
4. Bouddouch, A., Amaterz, E., Bakiz, B., Taoufyq, A., Guinneton, F., Villain, S., Gavarri, J-R., Valmalette, J-C. and Benlhachemi, A. *Nanotechnology for Environmental Engineering*, **2021**, *6*(1), 1-12.

NEW $CIGS_N$ LAMELLAR MATERIALS FOR PHOTO-INDUCED APPLICATIONS (PHOTOVOLTAICS AND PHOTO-CATALYSIS)

Amal BELHCEN[1], Maria Teresa CALDES[1], Catherine GUILLOT-DEUDON[1], Nicolas BARREAU[1], Helene BRAULT[1], Eric GAUTRON[1], Ludovic ARZEL[1], Adele RENAUD[2], Stephane JOBIC[1]

[1]- IMN, The Institute of Materials Jean Rouxel of Nantes, Nantes, France.
[2]- ISCR, Rennes Institute of Chemical Sciences, Rennes, France.
Amal.Belhcen1@cnrs-imn.fr, https://www.cnrs-imn.fr/

Recently, our research group has identified new $CIGS_n$ lamellar phases in the Cu_2S-In_2S_3-Ga_2S_3 system [1]. $CIGS_4$ ($Cu_{0.32}In_{1.74}Ga_{0.84}S_4$), $CIGS_5$ ($Cu_{0.65}In_{1.75}Ga_{1.4}S_5$) and $CIGS_6$ ($Cu_{1.44}In_{2.77}Ga_{0.76}S_6$) are interesting compounds looking to their optical gaps (see Figure 1) that can be comparable to those of the chalcopyrite $CuIn_{0.7}Ga_{0.3}S_2$, studied as potential absorber in a tandem solar cell and well represented in the emerging thin-film photovoltaic [2]. As it is shown in Figure 2 these materials present a 2D structure with generic compositions $(M_{(Td)})_{n-2}(In_{(Oh)})\ S_n$ (M = Cu, In, Ga), with cations in tetrahedral (Td) and octahedral (Oh) sulphur environments. All compounds exhibit a van der Waals gap (~3 Å).
The present work reports the further study of these new materials to identify their potential for photo-induced applications with a final objective of assembling a laboratory thin-film photovoltaic cell but also preparing these compounds with a suitable microstructure for photocatalysis.
Initially, intrinsic properties of the synthesized $CIGS_n$ lamellar compounds were determined and compared to those of the chalcopyrite ones. Therefore, the flat band potentials of $CIGS_n$ compounds were measured, aiming to optimise the heterojunction offsets, as a first step on bulk samples. The obtained results were compared to that of the chalcopyrite $CuIn_{0.7}Ga_{0.3}S_2$ which was estimated around -5.3 eV (see Figure 3).
The $CIGS_n$ lamellar samples were successfully synthesised as bulk samples using the ceramic route and as thin films by vacuum co-evaporation technique from elementary sources. Figure 4 shows an HAADF-STEM image of the scratched powder from a prepared thin film presented on the bottom of the figure. The measured distance between the octahedral In-S layers (observed as brighter lines) as well as chemical composition analysed by EDX, confirm that a $CIGS_5$ lamellar phase has been successfully deposited [3].
Other synthetic methods (microwaved-assisted solvothermal synthesis) also was carried out to adapt the microstructure. $CIGS_n$ nanocrystals were successfully prepared for the desired application, although the $Cu(Ga,In)S_2$ phase is detected as impurity, first catalytic tests will be undertaken soon.
Moreover, an anionic substitution study was implemented in order to find out if it is possible to keep the same lamellar structure while replacing sulphur by selenium and also to modulate the optoelectronic properties of the compounds.

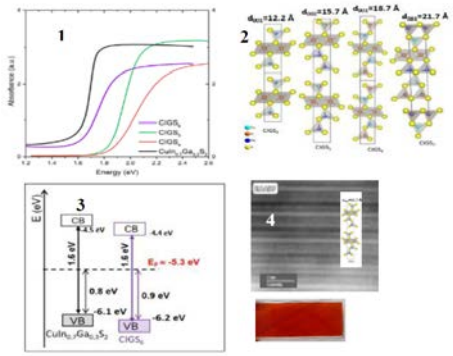

Figure: **1)** Kubelka-Munk transformed reflectance spectra of $CIGS_n$ and $CuIn_{0.7}Ga_{0.3}S_2$ compounds. **2)** $CIGS_n$ structure types. **3)** Sketch of the energy diagrams of $CIGS_6$ and of $CuIn_{0.7}Ga_{0.3}S_2$ chalcopyrite. **4)** HAADF-STEM image of $CIGS_5$ thin film.

[1] Caldes, M., Guillot-Deudon, C., Thomere, A., Penicaud, M., Gautron, E., Boullay, P., Bujoli-Doeuff, M., Barreau, N., Jobic, S. and Lafond, A., **2020**. Layered Quaternary Compounds in the Cu_2S–In_2S_3–Ga_2S_3 system. *Inorganic Chemistry*, 59(7), pp.4546-4553.
[2] Thomere, A., Guillot-Deudon, C., Caldes, M., Bodeux, R., Barreau, N., Jobic, S. and Lafond, A., **2018**. Chemical crystallographic investigation on Cu_2S-In_2S_3-Ga_2S_3 ternary system. *Thin Solid Films*, 665, pp.46-50.
[3] Funded by the French Contrat Plan État-Région and the European Regional Development Fund of Pays de la Loire, the CIMEN Electron Microscopy Center in Nantes is greatly acknowledged.

FROM CLUSTERS TO NANOSTRUCTURED TRANSITION METAL NITRIDES AND CARBIDES. *APPLICATION IN HETEROGEOUS CATALYSIS*

Franck Tessier[1], Kévin Guy[1,2,3], Guillaume Dubois[1], Fabien Grasset[1,3], Stéphane Cordier[1], Helena Kaper[2], Caroline Tardivat[2], Naoki Ohashi[3,4], Tetsuo Uchikoshi[3,4], David Lechevalier[3]

[1] *Univ. Rennes, CNRS, Institut des Sciences Chimiques de Rennes – UMR 6226, 35000 Rennes, France*

[2] *Ceramic Synthesis and Functionalization Laboratory, UMR 3080, SGR Provence-CNRS, 84306 Cavaillon, France*

[3] *CNRS - Saint-Gobain - NIMS, IRL 3629, Laboratory for Innovative Key Materials and Structures (LINK), National Institute for Materials Science, Tsukuba 305-0044, Japon.*

[4] *Research Center for Functional Materials, National Institute for Materials Sciences, Tsukuba, Japon*

Franck.Tessier@univ-rennes1.fr, iscr.univ-rennes1.fr

Keywords: clusters, nitrides, carbides, heterogeneous catalysis

Summary:

Transition metal nitrides/carbides form a class of materials with unique physicochemical properties, giving them a wide potential of applications, in particular in heterogeneous catalysis, in reactions traditionally catalyzed by noble metals [1].

Our collaboration within the consortium Université de Rennes 1 - CNRS - Saint-Gobain - IRL LINK (Tsukuba, Japan) is illustrated by recent results in the preparation of nanostructured transition metal nitrides and carbides from cluster compounds for the water gas shift reaction (WGSR: $CO + H_2O \rightarrow CO_2 + H_2$). The aim is to develop a less expensive alternative to platinum used as a catalyst. This reaction is used in particular upstream of fuel cells for vehicles in order to purify the dihydrogen supplying the cell.

This presentation will focus on the nitridation of the nanoscale precursor $(TBA)_2Mo_6Br_{14}$ [2] which leads at relatively low temperatures to Mo_2N and Mo_5N_6 nitrides with high specific surface areas. The study of the catalytic properties shows that the cluster route, compared to the classic oxide and sulfide routes [3], leads to higher CO / CO_2 conversion rates [4]. A similar approach between molybdenum clusters and sucrose or urea allows to extend this original process to the synthesis of nanostructured carbides.

References:

[1] Hargreaves J.S.J., Coord. Chem. Rev. **2013**, *257*, 2015-2031.
[2] Kirakci K., Cordier S., Perrin C., Z. Anorg. Allg. Chem. **2005**, *631*, 411-416.
[3] Marchand R., Tessier F., DiSalvo F.J., J. Mater. Chem. **1999**, *9*, 297-304.
[4] Guy K., Tessier F., Kaper H., Grasset F., Dumait N., Demange V., Nishio M., Matsushita Y., Matsui Y., Takei T., Lechevalier D., Tardivat C., Uchikoshi T., Ohashi N., Cordier S. Chem. Mater. **2020**, *32*, 6026-6034.

EVOLUTION OF CERIUM TRIHYDROXIDE $Ce(OH)_3$ IN AIR: TOWARD AN UNREPORTED CERIUM (OXY)HYDROXIDE PHASE?

Rémi F. ANDRE,[1] and Sophie CARENCO[1]

[1]*Laboratoire de Chimie de la Matière Condensée de Paris, Sorbonne Université/CNRS/Collège de France, Paris*
remi.andre@sorbonne-universite.fr, lcmcp.upmc.fr/site

Keywords: cerium oxide; cerium hydroxide; mixed valence; XANES; reactivity; Near ambient pressure-XPS

Summary: Cerium oxide is a well-known mixed valence oxide, used for a variety of catalytic reactions ranging from automobile exhaust to gas phase semi-hydrogenation of acetylene.[1] We report here a hydrothermal synthesis of $Ce(OH)_3$ and CeO_2 100 nm large nanoparticles by precipitating a cerium nitrate salt with KOH (Fig. 1). We studied the influence of several process parameters, in particular the gas phase of the reaction, on the final $Ce(OH)_3/CeO_2$ ratio, and could obtain XRD-pure $Ce(OH)_3$. We discovered by serendipity an unreported evolution in air of $Ce(OH)_3$ into a close crystal phase, not referenced in the databases. The "air aged $Ce(OH)_3$" contains $Ce^{(IV)}$ atoms but is different from CeO_2 and $Ce(OH)_4$. The material was characterized by means of X-ray Diffraction, Infrared spectroscopy, X-ray Absorption Spectroscopy and Transmission Electron Microscopy (Fig. 1A-C) in order to suggest a possible structure. We also proved a low temperature calcination (200 °C, 2 h, Ar) of this "air aged $Ce(OH)_3$" produces highly defective cerium oxide CeO_{2-x} nanoparticles.
We then investigated the interaction of the reduced cerium oxide CeO_{2-x} with H_2 (0.14 mbar) by Near Ambient Pressure – X-ray Photoelectron Spectroscopy (NAP-XPS). At 100 °C, the surface $Ce^{(III)}$ ratio decreases from 72 % to 48 % upon increasing H_2 pressure (Fig. 1D), interpretated as the formation of surface hydrides at oxygen vacancy sites. Such an oxidation of the surface $Ce^{(III)}$ atoms in $Ce^{(IV)}$ atoms by incorporation of H_2 is consistent with recent observations in the case of CeO_2 microparticles (from 9.2 % to 6.5 % for Freund *et al.*) but in a larger extent in our case.[2] Our result suggests that highly reactive mixed valence cerium oxide obtained through this controlled synthesis path could be of high interest to form surface hydride and thereby for hydrogenation catalysis.

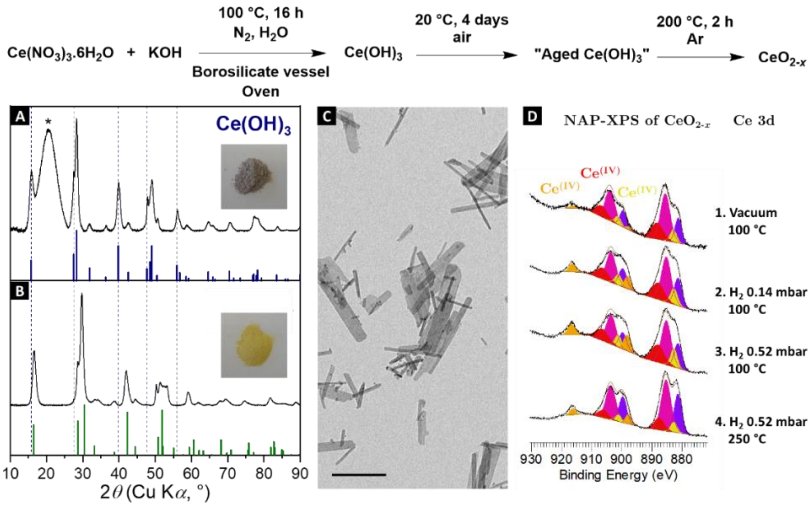

Fig. 1 Hydrothermal synthesis of $Ce(OH)_3$ and subsequent aging and calcination. (A) XRD pattern of fresh $Ce(OH)_3$. (B) XRD pattern of aged $Ce(OH)_3$ (green bars: $Tm(OH)_3$). (C) TEM image of the $Ce(OH)_3$ nanoparticles (the black bar represents 100 nm). (D) NAP-XPS spectra of reduced cerium oxide upon exposure to H_2 (orange component is associated to $Ce^{(IV)}$).

References:
1. Vilé, G.; Bridier, B; Wichert, J. and Pérez-Ramírez, J., *Angew. Chem. Int. Ed.* **2012**, *51* (34), 8620-8623
2. Li, Z.; Werner, K.; …; Huang, W.; Freund, H.-J., *Angew. Chem. Int. Ed.* **2019**, *58* (41), 14686-14693

EXPLORING ZINC-TEREPHTHALATE COMPLEXES THROUGH MULTI NUCLEAR SSNMR AND *IN-SITU* REACTION MONITORING BY RAMAN SPECTROSCOPY

C. Leroy[1], C. Gervais[2], T.-X. Métro[3], D. Laurencin[1]

[1]*ICGM, Univ Montpellier, CNRS, ENSCM, Montpellier, France*
[2]*LCMCP, UPMC Univ Paris 06, UMR 7574, Sorbonne Universités, Paris, France*
[3]*IBMM, Univ Montpellier, CNRS, ENSCM, Montpellier, France*
cesar.leroy@umontpellier.fr

Keywords: Mechanochemistry; Operando; MOF; Raman; ssNMR)

Summary: Mechanochemistry has shown impressive improvements in past decades for developing sophisticated materials such as pharmaceutical cocrystals, zeolite-based catalysts or metal-organic frameworks (MOFs).[1] The latter are elaborate porous materials exhibiting interesting applications in storage of fuels, capture of CO2, catalysis...[2] Being able to control the nature of MOFs synthesized under mechanochemical conditions thus appears as an important goal. In this context, recently, *in-situ* methods for mechano-synthesis, such as X-Ray diffraction under synchrotron beam or Raman spectroscopy, have emerged so that information about reaction rates and presence of intermediates are now becoming accessible.[3]
In this contribution, we have studied the formation of zinc-based MOFs using terephthalic acid as organic ligand. The observation of several intermediate phases was made possible by *in-situ* Raman spectroscopy during ball-milling synthesis (see Fig. 1 a)). Solid-state NMR spectroscopy was then used, along with FTIR, to obtain information about unknown structures observed during the synthetic route. ^{13}C chemical shifts were proven to be sensitive to the binding mode of the dicarboxylic acids on the zinc atoms, in line with previous studies. [4] Chemical shift differences up to 5 ppm (Fig. 1 b)) helped to distinguish between monodentate and bridging binding modes. Moreover, further structural information could be obtained through the use of 1D and 2D ^{17}O NMR experiments of enriched compounds (Fig 1c).

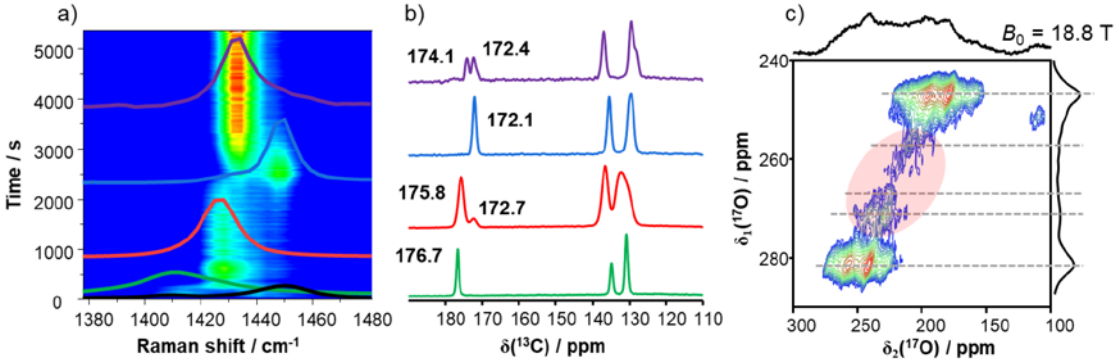

Figure 1. a) *In-situ* Raman spectroscopy of zinc terephthalates coordination complexes. b) ^{13}C ssNMR of the four different phases observed with Raman spectroscopy during the ball-milling synthesis. C) ^{17}O MQMAS spectrum of a ^{17}O-labeled zinc terephthalate compound.

[1] Friščić, T., et al., (2020). *Angew. Chem. Int. Ed.* **59**, 1018-1029.
[2] Furukawa, H., et al., (2013). *Science.* **341**, 1230444.
[3] Kulla, H., et al., (2018). *Angew. Chem. Int. Ed.* **57**, 5930-5933.
[4] Habib, H. A., et al., (2009). *Dalton. Trans.* **10**, 1742-1751.

3D PRINTED CELLULOSE NANOCRYSTALS BASED COMPOSITES: TOWARDS ROBUST BIOMIMETIC SCAFFOLDS FOR BONE REPAIR

Kanga M. N'GATTA[1,2], Habib BELAID[1,3], Marilyn KAJDAN[3], Edjia F. ASSANVO[b], David BOA[2], Vincent CAVAILLÈS[3], Mikhael BECHELANY[1], Chrystelle SALAMEH[1]

[1] *Institut Européen des Membranes, IEM-UMR 5635, ENSCM, CNRS, Univ Montpellier, Montpellier, France*

[2] *LTPCM, Laboratoire de Thermodynamique et de Physico-Chimie du Milieu, UFR SFA, Université Nangui Abrogoua, 02 BP 801 Abidjan 02, Côte d'Ivoire*

[3] *IRCM, Institut de Recherche en Cancérologie de Montpellier, INSERM U1194, Université Montpellier, Montpellier F-34298, France*
Kanga-marius.ngatta@umontpellier.fr

Keywords: Cellulose nanocrystals, Polylactic Acid, Fused Deposition Modelling, Scaffolds, Bone repair.

Summary: Cellulose nanocrystals (CNCs) are drawing increasing attention in the field of biomedical and smart healthcare due to their inherent sustainability, biocompatibility, biodegradability and high mechanical properties. In this research, plant fibres were extracted from *Ficus thonningii* (FT), naturally available in Côte d'Ivoire, treated with sodium hydroxide and hydrogen peroxide to remove hemicellulose and lignin and finally collected as cellulose. The collected cellulose was subjected to acid hydrolysis with sulphuric acid to obtain CNCs. The prepared nanocellulose was further characterised using Fourier transform infrared spectroscopy, X-ray diffraction and scanning electron microscopy to elucidate the chemical structure, crystallinity and morphology. Next, we fabricated 3D composite scaffolds based on polylactic acid (PLA) and extracted CNCs by fused deposition modelling (FDM) 3D printing technology and evaluated their biological performance. Scanning electron microscopy revealed that the printed scaffolds exhibit interconnected pores with an estimated average pore size around 400 µm and are therefore suitable for the viability, attachment, proliferation and differentiation of bone cells. X-ray diffraction confirmed the presence of CNCs. The incorporation of 3 wt % of CNCs in the composite improves the mechanical properties of PLA (Young's modulus increased by 27.5%) and surface roughness, while contributing to the improvement of wettability by a transition from the hydrophobic surface of PLA to a hydrophilic surface (contact angle with water decreased by 17.27%). The mineralisation process of the printed scaffolds using simulated body fluid (SBF) was performed and the nucleation of hydroxyapatite was confirmed. In addition, cytocompatibility tests reveal that PLA and PLA-CNCs composites are non-toxic and compatible with osteoblastic cells. Our design, based on rapid 3D printing of PLA-CNCs composites, combines the ability to control the architecture and ensure good mechanical and biological properties of the scaffolds promoting thus potential materials for applications in tissue engineering and regenerative medicine.

TUNING SIZE AND SHAPE FOR THE DESIGN OF INNOVATIVE THERANOSTIC IRON OXIDE BASED NANOPARTICLES ENSURING MULTIMODAL THERAPY

Barbara FREIS,[1,2] Celine KIEFER,[1] Sonia FURGIUELE,[3] Céline HENOUMONT,[2] Christine AFFOLTER-ZBARASZCZUK,[4] Damien MERTZ,[1] Sebastien HARLEPP,[4] Florent MEYER,[4] Fabrice JOURNE,[3] Sven SAUSSEZ,[3] Sophie LAURENT,[2*] Sylvie BEGIN-COLIN[1*]

[1]*Université de Strasbourg, CNRS, Institut de Physique et Chimie des Matériaux, ,Strasbourg, France*
[2]*Laboratoire de NMR et d'Imagerie Moléculaire, Université de Mons, Mons, Belgium*
[3]*Service d'Anatomie Humaine et d'Oncologie Expérimentale, Mons, Belgium*
[4]*Inserm U1121, Faculté de médecine, Strasbourg, France*

barbara.freis@ipcms.unistra.fr, http://www.ipcms.unistra.fr/

Keywords: iron oxide nanoparticles; theranostic; magnetic hyperthermia; photothermia; sonotherapy; MRI

Summary:
Designing nanoparticles (NPs) for targeted cancer diagnosis and therapy is currently one challenge in nanomedecine. Indeed new ways of diagnosis and treatments must be found to increase the survival rate of patients and to lessen the length of treatment for them. Iron oxide functionalized NPs are the most promising solution thanks to their theranostic property: they offer the possibility to both diagnose and treat the patient and then to follow the effect of therapy by imaging. Besides being T2 contrast agents for MRI, iron oxide NPs act as therapeutic agents by magnetic hyperthermia when correctly designed[1]. To be a good heating agent, iron oxide NPs have to display a high magneto-crystalline anisotropy and ways to increase it are to tune the NPs size and shape [1].Iron oxide NPs can also express an increased thermal response under laser irradiation [2] which is favourable for a combined therapy. Moreover, promising results shows that iron oxide NPs could be efficient sonosentisizers for anticancer treatment [3].

In that context, we have developed iron oxides NPs with different sizes and shapes by thermal decomposition method. The influence of the reaction temperature, the heating rate and the surfactant's nature on the NPs' size and shape was elucidated. In this way reproducible NPs with different shapes (plates, cubes and spheres) and with mean sizes in the range 5-25 nm were thus synthesized and coated with dendron molecules for biocompatibility. NPs' magnetic properties as well as their MRI properties were determined and the effect of the NPs size and shape on magnetic hyperthermia, photothermia and sonotherapy has been investigated both in suspension and in cells to establish the optimal NPs design to combine therapies.

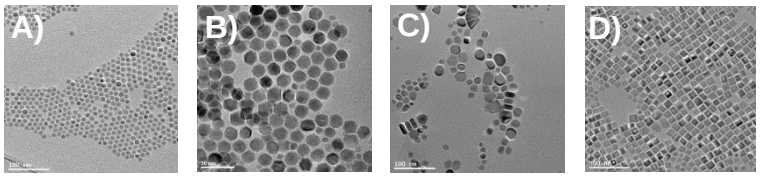

Fig. 1 TEM images of different iron oxide nanoparticules. A)10nm nanospheres; B) 19nm nanospheres, C) nanoplates (25nm long), D) nanocubes (25nm)

References:

1. Cotin, G; Kiefer, C; Perton, F; Ihiawakrim, D; Blanco-Andujar, C; Moldovan, S; Lefevre, C; Ersen, O; Pichon, B; Mertz, D; Bégin-Colin, S, *Nanomaterials*. **2018**, *8*, 881.
2. Espinosa, A; Kolosnjaj-Tabi, J; Abou-Hassan, A; Plan Sangnier, A; Curcio, A; Silva, A. K. A; Di Corato, R; Neveu, S; Pellegrino, T; Liz-Marzán, L. M; Wilhelm, C, *Adv. Funct. Mater*. **2018**, *28*, 1803660.
3. Fard, A; Zarepour, A; Zarrabi, A; Shaneia, A; Salehic, H, *Journal of Magnetism and Magnetic Materials***. 2015***, 394*, 44–49

NANOCOMPOSITE MEMBRANES BASED ON POLYMER/EXFOLIATED 2D MATERIALS OBTAINED BY PICKERING EMULSION

Bonito A. Karamoko [1,2], Damien Voiry [1], Chrystelle, Salameh [1], Kouassi B.Yao [2], Philippe Miele [1]

.[1] *Institut Européen des Membranes, ENSCM, CNRS, Université de Montpellier, France*
[2] *Laboratoire de Synthèse, Procédés Industriels, Environnement et Energies Renouvelables, Institut National Polytechnique Félix Houphouët-Boigny, Côte D'ivoire*

bonito.karamoko@enscm.fr

Keywords: Pickering emulsion, Polymer-derived ceramics, Graphene

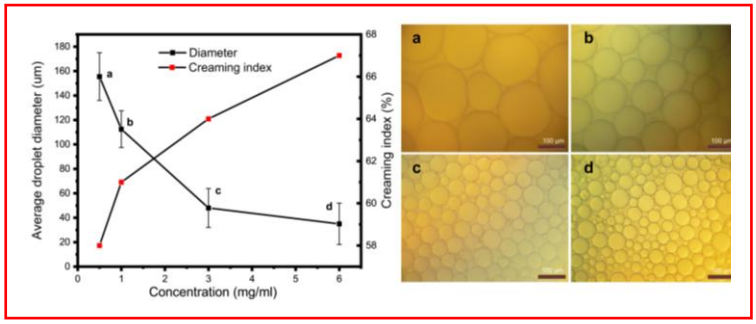

Driven by the growing need for potable water, water purification has become extremely important, yet very challenging. The use of non-oxide ceramic membranes for water treatment under harsh environments is witnessing a significant interest due to their high mechanical strength, structural stability and corrosion resistance at elevated temperatures[1].The Polymer-Derived ceramics (PDCs) route is an elegant strategy to obtain non-oxide ceramics from the pyrolysis of preceramic precursors with tailored composition, structure, shape and properties. The development of porous polymer-derived non oxide membranes for water filtration (such as SiC, SiCN) with both high flux and good selectivity remains very challenging. In this work, we propose to elaborate composite membranes by combining the PDCs route and 2D materials using the Pickering emulsions method. Because of the water sensitivity of the preceramic polymers, we developed an oil in oil Pickering emulsions strategy to prepare the composites[2]. Oil-in-Oil Pickering emulsions were obtained and used as soft template for the preparation of graphene-Si-based ceramic composites using DMSO and cyclohexane as oil phases. The different parameters that can influence the stability of such emulsions were studied in details.

Specifically, we examined the influence of the graphene concentration, time, emulsification rate, and DMSO/Cyclohexane volume ratio on the creaming index and the droplet size of the emulsion. Our systematic investigations showed that stable oil-in-oil Pickering emulsions based on preceramic polymers and 2D materials can be obtained. In my presentation i will highlight our results on the control of the droplet size and the creaming index.

References:

1. W, Wei., Z, Weiqi., J, Qian., X, Peng, Z, Zhaoxiang., Z, Feng., Xing, Weihong., *J. Memb. Sci.* **2017**,540, 381–390
2. B. Rodier, A. De Leon, C. Hemmingsen, and E. Pentzer, *ACS Macro Letters*, **2017**, 6 (11), 1201–1206.

TOPOCHEMICAL SULFUR DEINTERCALATION AND INTERCALATION IN RARE EARTH OXYSULFIDE COMPOUNDS FOR SYNTHESIS OF NEW METASTABLE MATERIALS

Louis-Béni Mvélé[1]

[1]*Institut des Matériaux Jean Rouxel, UMR6502, Nantes*

Keywords: Topochemical, deinsersion, sulfur, oxysulfide

Summary: Low-temperature synthesis is a developing field of solid-state chemistry, which provides access to metastable phases with new chemical properties and characteristics. The topochemical intercalation of the transition metal such as copper in the material $La_2O_2S_2$ leads to the synthesis of the known compound $La_2O_2Cu_2S_2$ [1]. The oxysulfide $La_2O_2S_2$ is formed by sulfur $(S_2)^{2-}$ dimers sandwiched between the $[La_2O_2]^{2+}$ layers, thus copper donates electrons to the sulfur dimers to form a two-dimensional layer in situ. However, when we use an alkali (Na, K, Rb) instead of copper, this one take out sulfur of $La_2O_2S_2$ by topochemical pathway and we observe the formation of the metastable compound OA-La_2O_2S with a structure different from the one of the stable variety. This PhD work aims to explore the topochemical deinsersion of sulfur of $Ln_2O_2S_2$ compounds (Ln = rare earth) and to compare their optical properties with those of their stable variants that give rise to many applications.

[1] Sasaki, S., Driss, D., et al (2018). A Topochemical Approach to Synthesize Layered Materials Based on the Redox Reactivity of Anionic Chalcogen Dimers. *Angewandte Chemie International Edition*, *57*(41), 13618-13623

GEO-INSPIRED PATHWAYS TOWARDS TERNARY NANOMATERIALS FOR ELECTROCATALYSIS

Daniel E. JANISCH[1], Edouard DE ROLLAND DALON[1], Fernando IGOA SALDANA[1], and David PORTEHAULT[1]

[1] *Sorbonne Université, CNRS, Laboratoire de Chimie de la Matière Condensée de Paris (LCMCP), 4 place Jussieu, F-75005 Paris, France*

daniel.janisch@sorbonne-universite.fr, https://lcmcp.upmc.fr/site/

Keywords: Nanomaterials, molten salts, *in situ* XRD, ternary phases, chemistry of silicon, boron

Summary: Nickel-metalloid compounds are emerging since 5 years as potential electrocatalysts of the hydrogen evolution reaction (HER) and the oxygen evolution reaction (OER)[1] involved in water splitting for H_2 production, as well as of the electrochemical reduction reaction of CO_2 (CO_2RR)[2].

In these compounds, the metalloids modify not only the charge density of the metal atoms, which are the catalytically active sites, but also the geometry of these surface sites due to the structural constrains imposed by the strong bonds between p-block atoms and metal atoms. To exacerbate the impact on electrocatalytic activity and product selectivity, we aim at combining not one but two metalloids, boron and silicon, with nickel, thus targeting ternary nickel silicoborides with unique crystal structures and new opportunities to tune the electronic structure. Silicoborides of transition metals are rare and their properties are unreported.[3] Hence, by targeting such materials, we not only aim at developing efficient electrocatalysts for a range of reactions, but we also aim at exploring new materials and their yet unknown properties.

The synthesis of metal silicoborides requires stringent conditions, including air-free conditions. More important, the high temperatures involved are detrimental to the isolation of nanomaterials, which are sought to increase the number of active sites per mass of catalyst, thus the catalytic activity. Inspired by geological processes like the crystallisation of rubies into deposits of salts, which were trapped and melted by plate tectonics in the earth's crust[4], we conceive laboratory scaled reactions to approximate and exploit similar conditions. At ambient pressure, inorganic molten salts allow for liquid-phase reactions in a wide temperature range (100 – 1000 °C). Precursors are mixed physically with the salts by milling and then heated above the melting point of the salt where the reaction will take place. The versatility of this liquid-mediated pathway offers a large range of experimental knobs whereby nucleation of nanoparticles is promoted and their growth is limited.[5]

We will present the synthesis of the ternary phase Ni_6Si_2B in the eutectic mixture LiCl-KCl from $NiCl_2$, that is reduced by Na_4Si_4 and $NaBH_4$. To understand reaction mechanisms and drive the exploration of composition and temperature ranges, we have developed a setup enabling *in situ* XRD measurements in molten salts. Following recent studies at ESRF beamline ID11, we could reveal the sequence of crystallization events towards the formation of Ni_6Si_2B within the molten salt. We especially revealed the intermediate formation of binary phases $Ni_{31}Si_{12}$ and Ni_2B, which subsequently reacted with each other to yield the ternary phase. We will show how this new knowledge can drive the optimisation of the nanomaterials and the exploration of new phases.

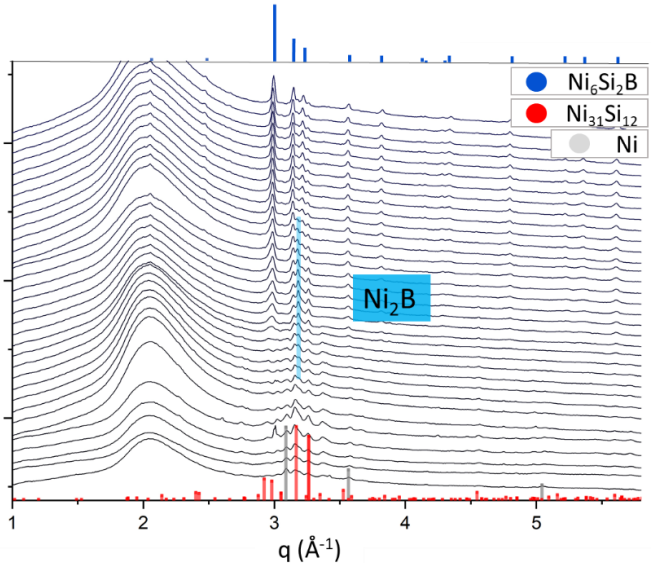

Fig 1: *In situ* XRD of the formation of Ni_6Si_2B in molten salts

References:

1. Masa, J. *et al.*, *Adv. Energy Mater.* **2019**, 9 (26), 1–8
2. Calvinho, K. *et al.*, *Energy Environ. Sci.* **2018**, 11 (9), 2550–2559
3. Lugscheider, E. *et al.*, *Monatshefte für Chemie* **1975**, 106 (5), 1155–1165
4. Giuliani, G. *et al.*, *Eur. J. Mineral.* **2015**, 27 (3), 393–404
5. Portehault, D. *et al.*, *Acc. Chem. Res.* **2018**, 51 (4), 930–939

FROM STACKED HOMO-LAYERS TO HETEROSTRUCTURES: PATHWAYS TO HYBRID LAYERED OXIDES

F. Payet,[1] C. Bouillet,[1] F. Leroux,[2] C. Leuvrey,[1] P. Rabu,[1] C. Taviot-Guého[2] and G. Rogez[1]

[1]*Institut de Physique et Chimie des Matériaux de Strasbourg, Strasbourg, France*
[2]*Institut de Chimie de Clermont-Ferrand, Clermont-Ferrand, France*
frederic.payet@ipcms.unistra.fr, https://www.ipcms.fr/frederic-payet/

Keywords: layered oxides; microwave-assisted functionalization; pyrenes; organosilane; nucleotides;

Summary: Two different approaches can be conducted when dealing with layered oxides, especially those with a perovskite-like structure. First, one can take advantage of the reactive interlayer space to insert or covalently graft molecular entities between the oxides slabs, leading to a hybrid layered material.[1,] In parallel, many works have been carried out to dissociate the inorganic oxide layers one from each other *i.e.* to exfoliate the layered material into nanosheets.[2] More recent works reveals the potentiality of coupling oxides nanosheets with another nano-objects to reach new properties.[3]

In our team, we combine both approaches, essentially on the layered oxide $H_2Bi_{0.1}Sr_{0.85}Ta_2O_9$ (HST). First, we hybridize this layered oxide with a large panel of molecules by microwave-assisted functionalization, which allows fast and efficient modification of HST.[1,] Then, we perform the exfoliation of the hybrid, resulting in functionalized oxide nanosheets. The delamination process is carried out in solution without any exfoliating agent while using mechanical shear-forces.[4] Finally, we aim at integrating such nanosheets into the form of nano-architectures. This latter step is mainly dependent on the molecular design of the inserted entities during functionalization.

We present here the synthesis of new hybrid layered oxides whose organic part might guide the building of nano-architectures. First, we modify the interlayer space of HST by organosilane derivatives which provides free amines at the surface of the oxide layer. Secondly, we graft pyrene derivatives on the inorganic layer: the resulting hybrid can be coupled with graphene or aromatic molecules *via* π-π interactions. Finally, we chose two complementary nucleotides, adenosine and thymidine, which can interact via specific hydrogen bonds. Their grafting into HST results in a hybrid material able to recognize specifically a surface or a nano-object exhibiting the complementary nucleobase at its surface. All the hybrid layered oxides are characterized by XRD, IR and NMR spectroscopies and electronic microscopy (**Figure 1**).

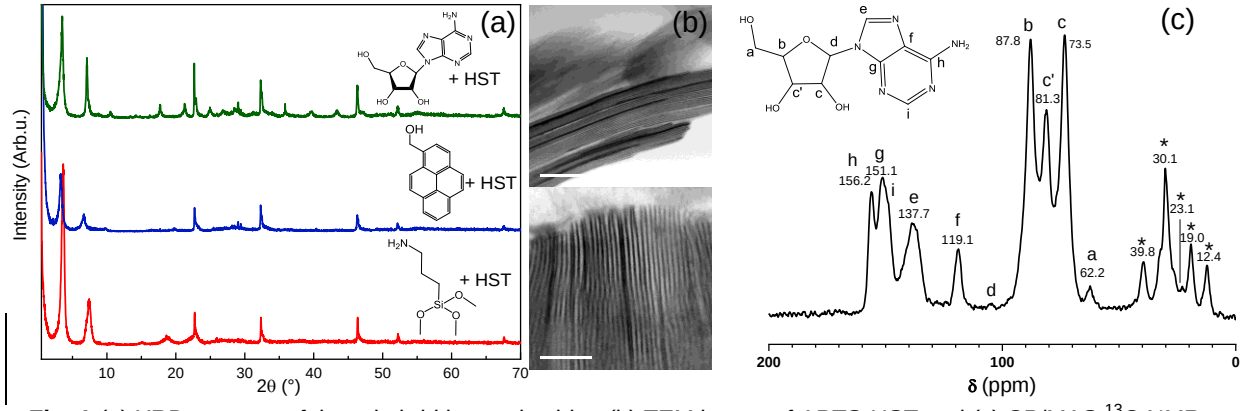

Fig. 1 (a) XRD patterns of three hybrid layered oxides (b) TEM image of APTS-HST and (c) CP/MAS ^{13}C NMR spectrum of Adenosine-HST.

References:
1. Wang, Y; Nikolopolou, M; Delahaye, E; Leuvrey, C; Leroux, F; Rabu, P; Rogez, G, *Chem. Sci.* **2018**, *9*, 7104-7114.
2. Tan, C; Cao, X; Wu, X-J; He, Q; Yang, J; Zhang, X; Chen, J; Zhao, W; Han,S; Nam; G-H; Sindoro, M; Zhang, H, *Chem. Rev*. **2017**, *117*, 6225-6331.
3. Timmerman, M; Xia, R; Le, P-T.P; Wang,Y; tenElshof, J-E, *Chem. Eur. J*. **2020**, *26*, 9084-9098.
4. Payet, F; Bouillet, C; Leroux, F; Leuvrey, C; Rabu, P; Schosseler, F ; Taviot-Guého, C ; Rogez, G, *J. Coilloid Interface Sci.* **2022**, *607*, 621-632.

MOLYBDATE FORMATION FROM SPENT FUEL DISSOLUTION: STUDY OF THE FIRST STAGE OF PRECIPITATION

E. Abi Rached[1,2], S. Costenoble[2], G. Stoclet[3], S. Grandjean[2] and M. Rivenet[1]

1 : Univ. Lille, CNRS, Centrale Lille, ENSCL, Univ. Artois, UMR 8181 – UCCS – Unité de Catalyse et Chimie du Solide, F-59000 Lille, France
2 : CEA, DES, ISEC, DMRC, Univ Montpellier, Marcoule, France
3 : Univ. Lille, CNRS, INRA, ENSCL, UMR 8207 - UMET - Unité Matériaux et Transformations, Lille, France

During the recycling of the spent nuclear fuel and more precisely during its dissolution in hot nitric acid prior to uranium and plutonium recover, a solid is formed and the precipitation leads to a fouling phenomenon that interferes with the proper functioning of the dissolution process. Structural and chemical analyses of the precipitate provide evidence that the chemical composition, crystalline structure and microstructure of the precipitate depend on the ageing time and tetravalent elements ratio contained in the medium solution. Three crystalline phases predominate $Ce_xZr_{(1-x)}Mo_2O_7(OH)_2(H_2O)_2$ ($x \leq 0.3$; $0\% \leq X_M \leq 50\%$), $[Zr_xCe_{(2-x)}Mo_3O_{12}(NO_3)_2(H_2O)_2].H_2O$ ($70\% \leq X_M \leq 100\%$), which can be considered as a reaction intermediate, and $[Zr_xCe_{(3-x)}Mo_6O_{24}(H_2O)_2].(H_2O)_2$ ($x \leq 0.4$; $90\% \leq X_M \leq 100\%$) with $X_M = \frac{M(IV)}{M(IV)+Zr(IV)}$ and M = Ce, Pu.
This actual work aims to study the first stage of precipitation of the above mentioned molybdate compounds and elucidate the influence of solution (X_M ratio, Te(VI) lack or content), on their formation mechanisms. X-ray Scattering was used to study the cluster's formation at the beginning of precipitation, then to determine the aggregate sizes (SAXS and USAXS: small and ultra-small angle X-ray scattering) and finally to access to the atomic scale (WAXS: wide-angle X-ray scattering). *In-situ* analyses were also performed in order to follow the solid evolution as a function of time. The resulting X-ray scattering spectra were then modelled using the building units taken from the crystalline structure of the precipitate.

At low Ce content the $Ce_xZr_{(1-x)}Mo_2O_7(OH)_2(H_2O)_2$ compounds start to precipitate in solution through the agglomeration of amorphous clusters of composition $Zr_7Mo_8O_{71}$ (R = 5.8 Å). Once the critical radius is reached $Ce_xZr_{(1-x)}Mo_2O_7(OH)_2(H_2O)_2$ crystallises. This result is intermediate between the two crystallisation mechanisms proposed so far in the literature which state that $Ce_xZr_{(1-x)}Mo_2O_7(OH)_2(H_2O)_2$ occurs through a two-steps reaction involving two monomers, $HMoO_4^-$ and $Zr(OH)_2^{2+}$, which form a stoichiometric complex that reacts with another Mo monomer, $HMoO_4^-$, to form a [complex 2:1], or that the formation of $Ce_xZr_{(1-x)}Mo_2O_7(OH)_2(H_2O)_2$ involves an amorphous film formation followed by the fixation, nucleation and growth of $Ce_xZr_{(1-x)}Mo_2O_7(OH)_2(H_2O)_2$ particles. For higher Ce content, the precipitation mechanism involves the formation of an intermediate compound and confirms the XRD results obtained as a function of time. A building unit, $CeMo_6NO_{28}$ (R = 3.9 Å), modelled from the reaction intermediate is first obtained and then transforms into $[Zr_xCe_{(3-x)}Mo_6O_{24}(H_2O)_2].(H_2O)_2$ with time.

The effect of tellurium is predominant at low cerium content where $Ce_xZr_{(1-x)}Mo_2O_7(OH)_2(H_2O)_2$ is replaced by an amorphous phase. In this domain, $Zr_{13}Mo_{16}O_{135}$ (R = 9.6 Å) fits well the experimental spectrum at large q but there are some discrepancies at small q. Two hypotheses can possibly explain the difference: either the presence of a mixture of aggregates and small particles or the presence of particles even larger than $Zr_{13}Mo_{16}O_{135}$. Further experiments are under study to be able to conclude.

IS THERE ANY DYNAMIC MAGNETIC DIMER IN Sr_2CrNbO_6 ORDERED DOUBLE PEROVSKITE?

Maneesha VARGHESE [1], Mathieu DUTTINE [1], Vivian NASSIF [2], Matthew SUCHOMEL [1], Manuel GAUDON [1], Olivier TOULEMONDE [1]

[1] *Institut de chimie de la matière condensée de Bordeaux, 87 Avenue du Docteur Schweitzer, 33608 Pessac, France*

[2] *Institut Laue-Langevin, 71 avenue des Martyrs, CS 20156, 38042 Grenoble, France*

maneesha.varghese@icmcb.cnrs.fr, https://www.icmcb-bordeaux.cnrs.fr/

Keywords: Ordered double perovskite, magnetism, dynamic dimer, spin glass, valence bond glass

Summary: Competing magnetic interactions in materials had always given rise to fascinating phenomena in the field of condensed matter.[1] Geometric magnetic frustration induced by the edge shared tetrahedra had been the reason behind the observance of exotic magnetic properties like spin liquid, spin ice, spin glass, valence bond solid, valence bond glass etc. in double perovskites.[2,3]

The main objective of our study on ordered double perovskite Sr_2CrNbO_6 is to investigate if these systems behave like a valence bond glass (VBG). Room temperature powder X-ray diffraction (PXRD) pattern showed that Sr_2CrNbO_6 crystallizes in the cubic space group, $Fm\bar{3}m$ with cell parameter, a = 7.8(1) Å with 44% ordering of Cr^{3+}/Nb^{5+}. This poor degree of ordering likely results from a metal-metal charge transfer observed from UV-vis-NIR spectroscopy. Temperature dependent Neutron Diffraction measurement showed no magnetic peak in Sr_2CrNbO_6 at 1.8K and a quadratic distortion of the octahedra increase with charges localization with temperature decrease. The magnetization measurements in zero field cooled/field cooled (ZFC/FCC) mode under 1T have been carried out. It shows two different regions at high and intermediate temperature suggesting a valence bond glass behavior in the intermediate temperature range along with a spin glass transition at low temperature.
In this presentation, complementary temperature Electron Paramagnetic Resonance and specific heat will be presented aiming to characterize this exotic intermediate state prior to spin glass in Sr_2CrNbO_6.

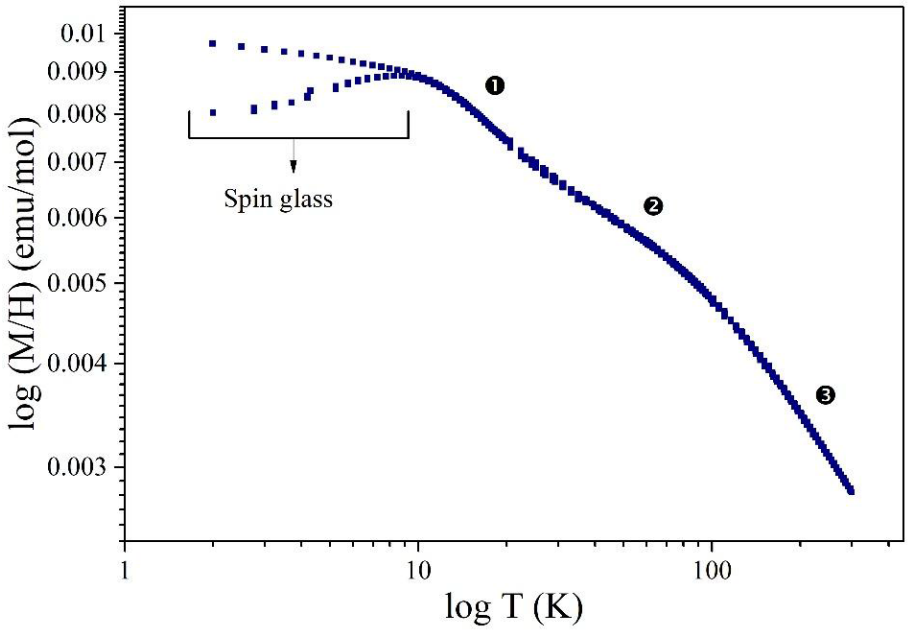

Fig 1: M/H vs T (logarithmic scale) plot of Sr_2CrNbO_6 double perovskite.

References:
[1] Hung-The, D. *Frustrated spin systems*. (World Scientific Publishing Co Pte Ltd, 2020)
[2] Phys. Rev. B **65**, 144413 (2002)
[3] Phys. Rev. B **81**, 224409 (2010)

INVESTIGATION OF MAGNETOELECTRIC PROPERTIES IN THE $Ni_{4-X}Co_XNb_2O_9$ SYSTEM

Jacqueline Nadine JIONGO DONGMO, [1] Françoise DAMAY, [2] Antoine MAIGNAN, [1]
Juan-Pablo BOLLETTA, [1] and Christine MARTIN[1]

[1]*Laboratoire CRISMAT, Normandie Univ, ENSICAEN, UNICAEN, CNRS, 14050 Caen, France*
[2]*Laboratoire Léon Brillouin, Université Paris-Saclay, CEA Saclay, 91191 GIF-SUR-YVETTE Cedex, France*
Jacqueline-nadine.jiongo-dongmo@ensicaen.fr

Keywords: Magnetoelectrics; transition metal oxides; crystalline structure; magnetism; diffraction

Summary: The 429 family (formula $M_4A_2O_9$, where M=Co, Mn, Fe, Mg and A=Nb or Ta) has a crystal structure derived from corundum [1], and represents an interesting class of materials because of its potential magnetoelectric (ME) properties [2-4]. While most compounds exhibit a substantial linear magnetoelectric effect (LME), such as $Co_4Nb_2O_9$ (electric polarization of 120 µC/m^2 in 7 T)[5], $Ni_4Nb_2O_9$ is characterized by a lack of magnetoelectricity[6]. Interestingly, $Co_4Nb_2O_9$ crystallizes in the trigonal *P*-3*c*1 space group with an antiferromagnetic transition at T_N=27K [7], when $Ni_4Nb_2O_9$ has an orthorhombic *Pbcn* crystal structure and exhibits a ferrimagnetic transition at T_N=76K [8]. The magnetic point group *m'm'm* associated with the *Pb'cn'* ferrimagnetic structure of $Ni_4Nb_2O_9$ does not allow magnetoelectric properties. We have initiated a study of the $Ni_{4-x}Co_xNb_2O_9$ series, to follow the structural and magnetic changes from $Ni_4Nb_2O_9$ to $Co_4Nb_2O_9$, and to check if it will be possible to generate magnetoelectric properties in the orthorhombic structure. This work relies on high temperature solid-state synthesis in air, X-ray and neutron diffraction experiments, combined with magnetization, dielectric and polarization measurements. Our results show that, for x ≤ 2.2, compounds exhibit a $Ni_4Nb_2O_9$–like behavior: orthorhombic structures with ferrimagnetic transition temperatures varying from 76K to 49K and lack of magnetoelectric effect. For x ≥ 2.5 a $Co_4Nb_2O_9$–like behavior is observed, i.e. trigonal structures with antiferromagnetic transition temperatures varying from 36K to 27K and magnetoelectric effect. The x=2.3 sample shows the coexistence of both phases and it is characterized by $Ni_4Nb_2O_9$–like magnetic properties and $Co_4Nb_2O_9$–like ferroelectric properties. Magnetic structures determination from x=2 to x= 3 is in progress.

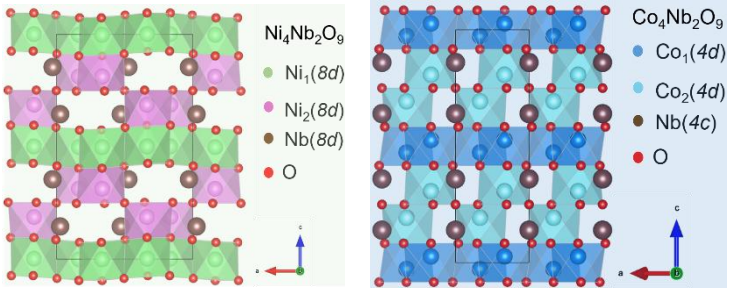

Fig. 1 $Ni_4Nb_2O_9$ vs $Co_4Nb_2O_9$

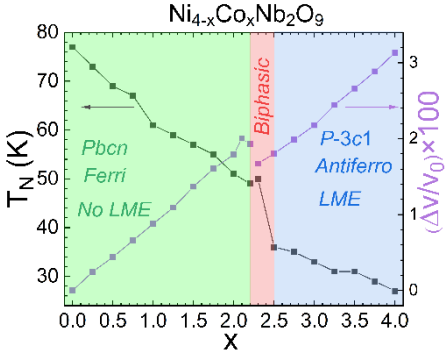

Fig. 2 Phase diagram of $Ni_{4-x}Co_xNb_2O_9$

References:
1. Bertaut, E. F.; Corliss, L.; Forrat, F.; Aleonard, R.; Pauthenet, R., *J. Phys. Chem. Solids* **1961**, *21* (3), 234–251.
2. Fang, Y.; Song, Y. Q.; Zhou, W. P.; Zhao, R.; Tang, R. J.; Yang, H.; Lv, L. Y.; Yang, S. G.; Wang, D. H.; Du, Y. W., *Scientific Reports* **2014**, *4* (1), 3860.
3. Maignan, A.; Martin, C., *Phys. Rev. B* **2018**, *97* (16), 161106.
4. Deng, G.; Cao, Y.; Ren, W.; Cao, S.; Studer, A. J.; Gauthier, N.; Kenzelmann, M.; Davidson, G.; Rule, K. C.; Gardner, J. S.; Imperia, P.; Ulrich, C.; McIntyre, G. J.,*Phys. Rev. B* **2018**, *97* (8), 085154.
5. Fang, Y.; Zhou, W. P.; Yan, S. M.; Bai, R.; Qian, Z. H.; Xu, Q. Y.; Wang, D. H.; Du, Y. W., *J. Appl. Phys.* **2015**, *117* (17), 17B712.
6. Tailleur, E.; Martin, C.; Damay, F.; Fauth, F.; Maignan, *J. Appl. Phys.* **2020**, *127* (6), 063902.
7. Fischer, E.; Gorodetsky, G.; Hornreich, R. M., *Solid State Communications* **1972**, *10* (12), 1127–1132.
8. Ehrenberg, H.; Wltschek, G.; Weitzel, H.; Trouw, F.; Buettner, J. H.; Kroener, T.; Fuess, H., *Phys. Rev. B* **1995**, *52* (13), 9595–9600.

MANIPULATION OF THE ANIONIC AND CATIONIC SUB-LATTICES OF PYROCHLORES

Edouard Boivin[1], Frédérique Pourpoint[1], Sébastien Saitzek[1], Marielle Huvé[1], Pascal Roussel[1], Houria Kabbour[1]

[1] Univ. Lille, CNRS, Centrale Lille, ENSCL, Univ. Artois, UMR 8181-UCCS-Unité de Catalyse et Chimie du Solide, F-59000 Lille, France

Keywords: mixed anion compounds, band gap engineering, water splitting photocatalysis

Historically, the optimization of oxides physical properties has mainly been realized by cationic substitutions leading to moderate chemical alterations (control of the valence states, control of the anionic vacancies…) while the anionic substitutions strongly impact the chemical bonding (iono-covalency, polarizability, geometry…).[1] For photocatalysis applications, the anionic mixing allows to finely control the photon absorption and electron-holes transport properties thanks to band gap and local symmetry engineering.[2,3] Although numerous derivatives exist, the pyrochlore $A_2B_2X_6X'$ structure is often described as two interlocked sublattices, A_2X' and B_2X_6, with an anionic site, X' (8b Wyckoff position of the Fd-3m space group, X'= O, N, F, S and/or □…), possessing a large versatility towards the anionic diversity while the X site (48f position, X= O, F or S) has almost always been reported as mono-anionic (**Figure 1a**).[4] During this talk, through several new oxysulfides $A_2B_2O_5S_1□_1$ and oxyfluorides $A_2B_2O_5F_2$ (with A= Na^+ and/or ½ Sn^{2+} and B= Nb^{5+} or Ta^{5+}) characterized by powder XRD and solid state NMR (^{23}Na and ^{19}F), unusual anionic distributions will be addressed (**Figure 1b**).

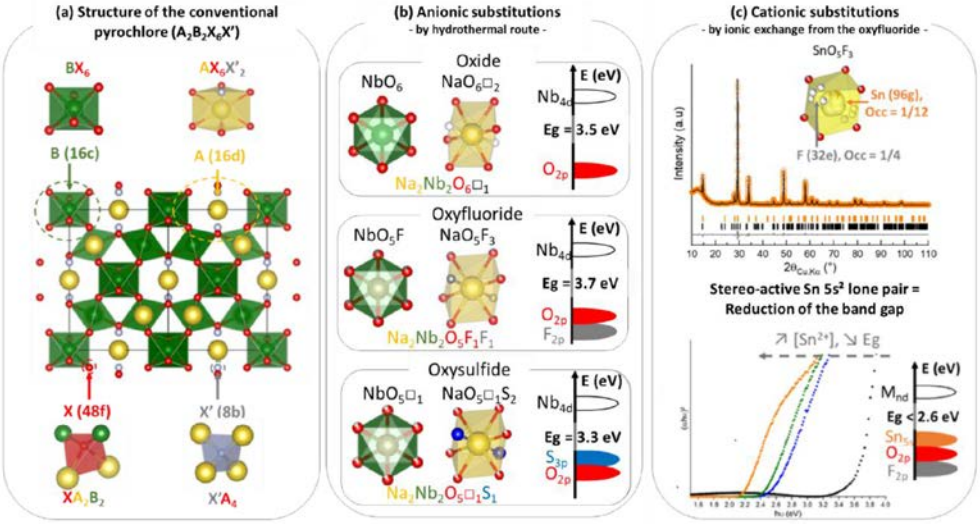

Figure 1: (a) structure of the conventional pyrochlore in the Fd-3m space group as well as the new derivatives obtained by manipulation of the (b) anionic and (c) cationic sublattices. The electronegativity of the anions and the stereo-activity of the Sn 5s² lone pair allow the fine control of the band gap.

Moreover, the Na^+/Sn^{2+} cationic exchange, from $Na_2M_2O_5F_2$ (M=Nb, Ta), leads to new metastable phases, $Na_{2-2x}Sn_x□_xM_2O_5F_2$, in which the unusual anionic distribution is preserved. Here, the Sn 5s² lone pair stereo-activity, the local $Sn^{2+}/Na^+/□$ ordering and the anionic mixing confer to these materials unprecedented crystallographic features as well as remarkable physical properties (**Figure 1c**). Indeed, the stereo-active lone pair of Sn^{2+}, located at the top of the valence band, massively reduces the band gap and hence promotes the visible light absorption which, in return, considerably enhances the photoconduction response and makes these materials suitable for overall water splitting photocatalysis under visible light irradiation.

1. Kageyama, H. *et al. Nat. Commun.* **2018**, 9(772) 1-15.
2. Kabbour, H. *et al. Chem. Commun.* **2020**, 3, 1645–1648.
3. Vonrüti, N. *et al. J. Mater. Chem. A.* **2019**, 7, 15741–15748.
4. Talanov, M. V. *et al. Chem. Mater.* **2021**, 33, 2706–2725.

AQUEOUS SOLUTION GROWTH AT 200°C AND CHARACTERIZATIONS OF PURE, ^{17}O- AND D-BASED HERBERTSMITHITE $ZnCu_3(OH)_6Cl_2$ SINGLE CRYSTALS

Vijaya Shanthi Paul Raj,[1] Matias Velazquez,[1] Alexandra Peña,[6] Marc Verdier,[1] Jean-Sébastien Micha,[7] Fabrice Bert,[3] Philippe Mendels,[3] Dominique Denux,[2] Philippe Veber,[4] Michel Lahaye,[5] and Christine Labrugère[5]

[1]*Univ. Grenoble Alpes, CNRS, Grenoble INP, SIMAP UMR 5266, 1130 rue de la piscine, Saint Martin d'Hères*
[2]*ICMCB, UMR 5026 CNRS-Université de Bordeaux-Bordeaux INP, 87 avenue du Dr. A. Schweitzer, Pessac*
[3]*Laboratoire de Physique des Solides, CNRS, Univ. Paris-Sud, Université Paris-Saclay, Orsay*
[4]*Université Lyon, Université Claude Bernard Lyon 1, CNRS, Institut Lumière Matière UMR 5306, Villeurbanne*
[5]*PLACAMAT, UMS 3626, CNRS-Université Bordeaux, 87 av. Albert Schweitzer, Pessac*
vijaya.paul@simap.grenoble-inp.fr

Spin liquids represent an exotic class of quantum matter where, despite strong exchange interactions, spins do not order or freeze down to zero temperature [1,2]. In 2D, this physics is represented by the famous example of the **K**agome **H**eisenberg **A**nti**F**erromagnetic (KHAF) Hamiltonian. On the Kagome lattice, frustrated triangles share corners and there is a consensus that the threefold combination of such a reduced connectivity, of S=1/2 spins and of frustration leads to a **Q**uantum **S**pin **L**iquid (QSL) state with fractional excitations. Herbertsmithite $ZnCu_3(OH)_6Cl_2$ is the first true and now emblematic QSL [3]. We have investigated the influence of temperature and temperature cycling on the growth rate, volume and $CuZn_x$ antisite disorder of the as grown single crystals by characterizing them with powder XRD, XPS, EPMA/WDS, ICP/AES, coupled TGA-MS and magnetic susceptibility. The morphology of the crystals were observed by optical microscopy and natural faces were indexed by the Laue method. Correlation between the $CuZn_x$ antisite disorder and the c-lattice parameter was also established. Besides, a more recent ^{17}O NMR study [4] shows that $ZnCu_x$ point defects in the Kagome triangles also exist, giving rise to spin dimers and singlet state with an almost null magnetic susceptibility. The solid solution developed formula may be written as $(Zn_{x-\delta'}Cu_{\delta'})(Cu_{4-x-\delta}Zn_{\delta})(^{17}OH)_6Cl_2$. In the ^{17}O-enriched crystal investigated, we have x=0.93, δ≈0.24 and δ'≈0.25. An upper bound for the hyperfine and exchange interactions distributions arising from disorder in this solid solution is $\Delta A/A \sim \Delta J/J \approx 3.6\%$ [4], and an upper bound estimate of the x = 0.93 composition crystal's mosaïcity could be performed by applying the magnetic field (and orienting the crystal) along **c**: 2°.We have run several experiments in order to determine the growth mechanism(s) involved in solution growth, as a function of pH, T and initial $[ZnCl_2]$ concentrations. Surface morphology of the as grown crystals were investigated by DIC/TIC and AFM microscopies and complimented by synchrotron micro-Laue diffraction and micro-XRF spectroscopy. On one hand, the power law analysis of height-difference correlation functions, obtained from AFM images of crystal surfaces, can often reveal the dominant growth mechanism involved in the crystal-solution interface motion. Meanwhile, synchrotron micro-Laue experiment from ESRF, which is unique in Europe having good angular (~1°) and spatial resolutions (200 nm), allows determining crystallographic orientation and morphological features on the growth interface. Hence, we have obtained our first results concerning the visualization and study of different morphological features of Herbertsmithite single crystals grown with different conditions. Triangles, including "wedding cake"-like mounds, rods, hexagon, several macrosteps, step bunching and large terraces have been observed.

[1] L. Balents, Spin liquids in frustrated magnets, *Nature*, **464**, 199 (2010).
[2] J. R. Chamorro, T. M. McQueen, T. T. Tran, Chemistry of Quantum Spin Liquids, *Chem. Rev.*, 121 (5) (2021) 2898-2934.
[3] M. Shores, E. Nytko, B. Barlett and D. Nocera, A structurally perfect S=1/2 Kagomé Antifferomagnet, *J. Am. Chem. Soc.*, **127**, 13462 (2005).
[4] P. Khuntia, M. Velazquez, Q. Barthélemy *et al.* Gapless ground state in the archetypal quantum kagome antiferromagnet $ZnCu_3(OH)_6Cl_2$. *Nat. Phys.*, (2020). https://doi.org/10.1038/s41567-020-0792-1

SYNTHESIS, CRYSTAL-STRUCTURE AND PHYSICAL PROPERTIES OF THE INFINITE LAYER PHASE OF BULK NICKELATES

Hassan D. Dahab[1], Alain Largetau[1], Nicolas Penin[1], Anthony Chiron[1], Etienne Durand[1], Pierre Rodière[2], Baptiste Vignolle[1] and Alain Demourgues[1]

[1]*Univ. Bordeaux, CNRS, Institut de Chimie de La Matière Condensée de Bordeaux, UMR 5026, Pessac, France*
[2]*Institut NÉEL, CNRS, Univ. Grenoble Alpes, Grenoble, France*
hassan.dahab@icmcb.cnrs.fr, , www.icmcb-bordeaux.cnrs.fr

Keywords: Nickelates; superconductivity; thin films; bulk; physical properties

Summary: The existence of a superconducting phase in infinite-layer Nickelates has been predicted twenty years ago in $LaNiO_2$ [1] but has remained elusive until the discovery in 2019 of a superconducting state in thin films of Sr-doped $NdNiO_2$ ($Nd_{0.8}Sr_{0.2}NiO_2$)[2]. This major breakthrough suggests the existence of a new family of unconventional superconductors. The crystal structure of these infinite-layer Nickelates consists in a stacking of NiO_2 layers separated by rare-earth spacer layer, stabilizing the unusual Ni^{1+} oxidation state, corresponding to $3d^9$ electronic configuration. Although superconductivity develops at quite low temperature (Tc ~ 9-15K[3]) at atmospheric pressure, the application of 12 GPa has been reported to boost Tc up to 31 K[4]. The similarity of the crystal structure and the electronic configuration $3d^9$, between the cuprates and the infinite layer Nickelates questions the ubiquity of the mechanism responsible for the occurrence of superconductivity. It should be emphasized that superconductivity has so far only been reported in ***epitaxial thin film*** of hole-doped $RENiO_2$ (RE = Nd, La, Pr) grown on $SrTiO_3$ substrate, the substrate stabilizing and straining the thin film. Therefore, it is yet unclear whether or not the epitaxial structure is necessary to obtain superconductivity. During this presentation, after a brief review on the discovery of superconductivity in the Nickelates, I will present the two-step synthesis protocol that we have developed in Bordeaux to produce bulk, polycrystalline powder. In a first step, Sr-doped $NdNiO_3$ polycrystalline samples are obtained by innovative synthesis route, using sol-gel method and high pressure of O_2. Careful analysis of XRD patterns allows the solubility limit of Sr in the perovskite phase to be determined. In a second step, a topochemical reduction of the perovskite phase using CaH_2 yields the infinite-layer phase. I will then report on the crystal structure of the infinite layer phase obtained by XRD and on the physical properties of the synthetized samples.

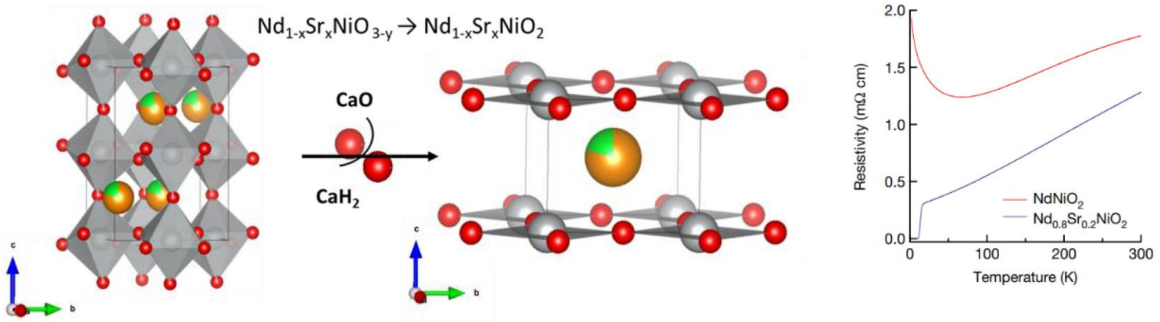

Fig. 1: Structures of $Nd_{0.8}Sr_{0.2}NiO_3$ (left), $Nd_{0.8}Sr_{0.2}NiO_2$ (reduced phase), resistivity measurements (from ref.2) versus temperature ρ(T) of the $Nd_{0.8}Sr_{0.2}NiO_3$ and $Nd_{0.8}Sr_{0.2}NiO_3$ in thin films.

References:
[1] Anisimov, V. I.; Bukhvalov, D.; Rice, T. M. *Phys. Rev. B* **1999**, *59* (12), 7901–7906.
[2] Li, D.; Lee, K.; Wang, B. Y.; Osada, M.; Crossley, S.; Lee, H. R.; Cui, Y.; Hikita, Y.; Hwang, H. Y.. *Nature* **2019**, *572* (7771), 624–627.
[3] Li, D.; Wang, B. Y.; Lee, K.; Harvey, S. P.; Osada, M.; Goodge, B. H.; Kourkoutis, L. F.; Hwang, H. Y. *Phys. Rev. Lett.* **2020**, 6.
[4] Wang, N. N.; Yang, M. W.; Chen, K. Y.; Yang, Z.; Zhang, H.; Zhu, Z. H.; Uwatoko, Y.; Dong, X. L.; Jin, K. J.; Sun, J. P.; Cheng, J.-G. *ArXiv210912811 Cond-Mat* **2021**

CHEMICAL DESIGN OF IrS_2 POLYMORPHS TO UNDERSTAND CHARGE/DISCHARGE ASYMMETRY IN ANIONIC REDOX SYSTEMS

Thomas Marchandier,[1,2,3] Sathiya Mariyappan,[1,2] Artem M. Abakumov,[4] Stéphane Jobic,[5] Bernard Humbert,[5] Jean-Yves Mevellec,[5] Gwenaëlle Rousse,[1,2,3] Maxim Avdeev,[6,7] Rémi Dedryvère,[2,8] Dominique Foix, [2,8] Antonella Iadecola,[2] Marie Liesse Doublet[2,9] and Jean-Marie Tarascon[1,2,3]

[1]*Collège de France, Chaire de Chimie du Solide et de l'Energie, UMR 8260, Paris, France*
[2]*Réseau sur le Stockage Electrochimique de l'Energie (RS2E), Paris, France*
[3]*Sorbonne Université, Paris, France*
[4]*Center for Energy Science and Technology, Skolkovo Institute of Science and Technology, Moscow, Russia*
[5]*Université de Nantes, CNRS, Institut des Matériaux Jean Rouxel, IMN, Nantes, France*
[6]*School of Chemistry, the University of Sydney, Sydney, Australia*
[7]*Australian Centre for Neutron Scattering, Australian Nuclear Science and Technology Organisation, New Lucas Heights, Australia*
[8]*PREM, CNRS, Université de Pau & Pays Adour, E2S-UPPA, Pau, France*
[9]*Institut Charles Gerhardt, Université de Montpellier-CNRS-ENSCM, Montpellier, France*
thomas.marchandier@college-de-france.fr, https://solid-state-chemistry-energy-lab.org/

Keywords: Li-ion batteries, Intercalation chemistry, Anionic redox

Summary: Li-ion batteries are growing in demands and such growth calls for the quest of high energy density electrode materials.[1] Li-rich layered oxides ($Li_{1+x}M_{1-x}O_2$ where M stands for transition metal ion(s)) show both cationic and anionic redox are expected to meet the high energy requirement. However, the oxygen anion activity triggers numerous structural and electronic rearrangements that need to be understood prior envisioning applications.[2] In particular, the understanding of voltage hysteresis is paramount because it questions the symmetry of redox processes between charge and discharge. Nevertheless, no common consensus has been reached yet on its origin[3],[4] and most of the scenarios are based on techniques whose interpretation is difficult and rarely leads to unanimous conclusions, especially on the nature of oxidized anionic species.

One naive strategy to clarify reversible asymmetry processes upon cycling is to study simple systems where migrated cations or anionic dimers could be clearly stabilized and identified. Sulfides, that are known to easily stabilize oxidized sulfur species such as S-S dimers, are obvious candidates. This phase that combines both sulfur dimers and a ramsdellite-like open framework is suitable for lithium topotactic insertion.[6] Moreover, intrigued by the possibility to form lithiated iridium sulfides, we managed to stabilize a high temperature $LiIrS_2$ phase isostructural to $LiTiS_2$. Interestingly, in spite of similar chemical compositions, $LiIrS_2$ and IrS_2 materials show completely different electrochemical behaviors (cf. fig 1 a). By combining diffraction techniques (synchrotron XRD, neutron powder diffraction (NPD)), high resolution TEM and spectroscopic analyses (XAS, XPS or Raman spectroscopies), we show that the lithiation reaction in both Li_xIrS_2 systems proceeds through different structural and electronic pathways (cf. fig 1 b). This study reveals the implications of the structure and of the dimers upon reaction pathways and then gives valuable insights for understanding better the hysteresis in anionic redox systems.

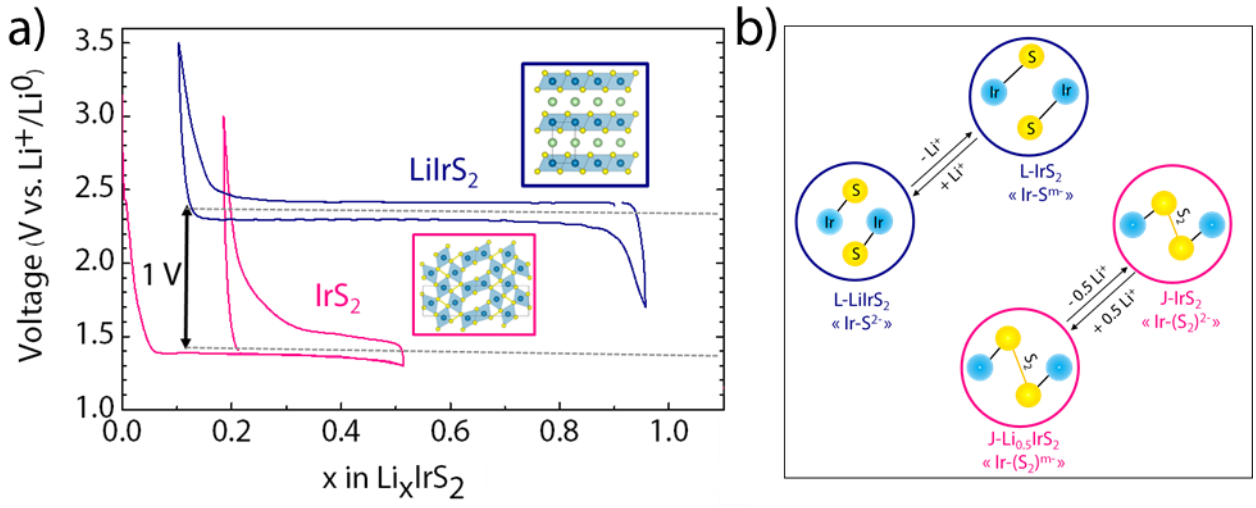

Fig. 1 a) First cycle voltage−composition trace of $LirS_2$ (blue) and IrS_2 (pink) cycled at C/20 (1 Li inserted or extracted in 20 h). b) Schematic drawing of the charge compensation in both J- and L-Li_xIrS_2 polymorphs.

References:

1. Armand, M; Tarascon, J.-M, *Nature.* **2001**, 414 (November), 359–367.
2. Assat, G.; Tarascon, J. M. *Nat. Energy.* **2018**, 3 (5), 373–386.
3. Gent, W. E.; Lim, K.; Liang, Y.; Li, Q.; Barnes, T.; Ahn, S. J.; Stone, K. H.; McIntire, M.; Hong, J.; Song, J. H.; Li, Y.; Mehta, A.; Ermon, S.; Tyliszczak, T.; Kilcoyne, D.; Vine, D.; Park, J. H.; Doo, S. K.; Toney, M. F.; Yang, W.; Prendergast, D.; Chueh, W. C., *Nat. Commun*. **2017**, 8 (1).
4. Jacquet, Q.; Iadecola, A.; Saubanère, M.; Li, H.; Berg, E. J.; Rousse, G.; Cabana, J.; Doublet, M. L.; Tarascon, J. M., *J. Am. Chem. Soc*. **2019**, 141 (29), 11452–11464.
5. Rouxel, J, *Chem. - A Eur. J.* **1996**, 2 (9), 1053–1059.
6. Jobic, S.; Deniard, P.; Brec, R.; Rouxel, J.; Drew, M. G. B.; David, W. I. F., *J. Solid State Chem.* **1990**, 89, 315–327.

MACHINE-LEARNING-ASSISTED DISCOVERY OF NEW THERMOELECTRIC OCTAHEDRAL TRANSITION-METAL CLUSTER CHALCOGENIDES

Isaac Chantrenne,[a] Fabien Grasset,[a] Stéphane Cordier,[a] David Berthebaud,[b] Guillaume Lambard,[c] Bruno Fontaine,[a] Régis Gautier[a] and Jean-François Halet[b]

[a]*Univ Rennes, ENSC Rennes, CNRS, Institut des Sciences Chimiques de Rennes – UMR 6226, Rennes, France*
[b]*CNRS – Saint-Gobain – NIMS, Laboratory for Innovative Key Materials and Structures (LINK) - IRL 3629, National Institute for Materials Science (NIMS), Tsukuba 305-0044, Japan*
[c]*CMI2 – MaDIS, National Institute for Materials Science (NIMS), Tsukuba 305-0047, Japan*

Since their discovery in the earliest 70's, Chevrel-Sergent phases ($M_xMo_6X_8$; M = Ag, Sn, Ca, Sr, Ba, Sn, Pb, 3d elements or lanthanides; X = S, Se, or Te; x = 0−4) [1] have been extensively studied, mainly for their superconducting properties [2], but also for other various applications in magnetic devices, catalysis, batteries or thermoelectricity [3]. Later, some derivative phases were found, containing larger clusters such as Mo_9X_{11} or $Mo_{30}X_{32}$ resulting from one-dimensional *trans*-face sharing of Mo_6 octahedra [4]. Some of them, such as $Ag_xMo_9Se_{11}$ (x = 3.6 – 3.8), show outstandingly low lattice thermal conductivity, giving rise to promising thermoelectric properties [5]. With these results in mind, electronic structure and electronic transport DFT calculations and machine learning approaches are used for the design of new cluster species which could display interesting thermoelectric properties. The first results will be presented.

References

[1] R. Chevrel, M. Sergent, J. Prigent, *J. Solid State Chem.,* **1971**, *3*, 515-519.
[2] T. Matthias, M. Marezio, E. Corenzwit, A.S. Cooper, H.E. Barz, *Science,* **1972**, *175*, 1465-1466.
[3] T. Caillat, J.-P. Fleurial, G. J. Snyder, *Solid State Sci*. **1999**, *1*, 535-544.
[4] a) S. Picard, J.-Y. Saillard, P. Gougeon, H. Noël, M. Potel, *J. Solid State Chem.*, **2000**, *155*, 417-426. b) P. Gougeon, P. Gall, A. Huguenot, R. Al Rahal Al Orabi, R. Gautier, *Inorg. Chem*, **2019**, *58*, 22, 15236-15245.
[5] a) P. Gougeon, J. Padiou, J.Y. Le Marouille, M. Potel, M. Sergent, *J. Solid State Chem.*, **1984**, *51*, 2, 218-226. b) R. Al Rahal Al Orabi, B. Boucher, B. Fontaine, P. Gall, C. Candolfi, B. Lenoir, P. Gougeon, J.-F. Halet, R. Gautier, *J. Mater. Chem. C*, **2017**, *5*, 12097-12104. c) C. Candolfi, P. Gougeon, P. Gall, M. Potel, A. Dauscher, B. Lenoir, *Structure and Bonding*, **2019**, *180*, 125-141.

SYNTHETIC $CuPbBi_5S_9$: A SEMI-ORDERED CATION DEFICIENT AIKINITE KEY-METRIX FOR HIGH THERMOELECTRIC PERFORMANCES

Krishnendu Maji,[1] Pierric Lemoine,[2] Adèle Renaud,[2] Bin Zhang,[3,4] Xiaoyuan Zhou,[3,4] Virginia Carnevali,[5] Christophe Candolfi,[6] Bernard Raveau,[1] Rabih Al Rahal Al Orabi,[5] Marco Fornari,[5] Paz Vaqueiro,[7] Mathieu Pasturel,[2] Carmelo Prestipino,[2] Denis Menut,[8] Emmanuel Guilmeau[1*]

[1]*CRISMAT, CNRS, Normandie Univ, ENSICAEN, UNICAEN, 14000 Caen, France*
[2]*Univ Rennes, ISCR – UMR 6226, CNRS, F-35000 Rennes, France*
[3]*College of Physics and Institute of Advanced Interdisciplinary Studies, Chongqing University, Chongqing 401331, China*
[4]*Analytical and Testing Center of Chongqing University, Chongqing 401331, China*
[5]*Department of Physics and Science of Advanced Materials Program, Central Michigan University, Mt. Pleasant, MI 48859, USA*
[6]*Institut Jean Lamour, UMR 7198 CNRS – Université de Lorraine, 2 allée André Guinier-Campus ARTEM, BP 50840, 54011 Nancy Cedex, France*
[7]*Department of Chemistry, University of Reading, Whiteknights, Reading, RG6 6AD, United Kingdom*
[8]*Synchrotron SOLEIL, Ligne MARS, L'Orme des Merisiers, Saint Aubin, 91192 Gif-sur-Yvette, France*
krishnendu.maji@ensicaen.fr, https://crismat.cnrs.fr/

Keywords: Gladite, Sulfide, Thermoelectric, Mechanical alloying

Summary: A highly pure semi-ordered cation deficient aikinite mineral type $CuPbBi_5S_9$ has been synthesized by combining mechanical alloying and SPS techniques. This synthetic sulphide, though it exhibits characteristics of a highly resistive degenerate semi-conductor (r ~ 5.103 Ω cm and S ~ 1300 µV/K at 400K) and of a poor thermoelectric (ZT ~ 0.04 at room temperature) is revealed to be an exceptional matrix for generating high thermoelectric performances by doping with Cl or an excess of Bi, leading to a thermoelectric figure of merit of 0.30 - 0.43 at 700 K (Fig. 1).[1] The low thermal conductivity of these sulphides is also explained by the fact that their structure is essentially built up of heavy $6s^2$ lone pair cations, Bi^{3+} and Pb^{2+}, and shows significant cationic disordering. It is worth pointing out that the present compound which represents the member x = 1/3 of a large series of closely related sulphides $(Cu_{1-x}\square_x)Pb_{1-x}Bi_{1+x}S_3$ with $0 \leq x \leq 1$ opens the way for the investigation of a broad field of thermoelectric materials by varying the chemical composition and by controlling the order-disorder phenomena in this system.[2,3]

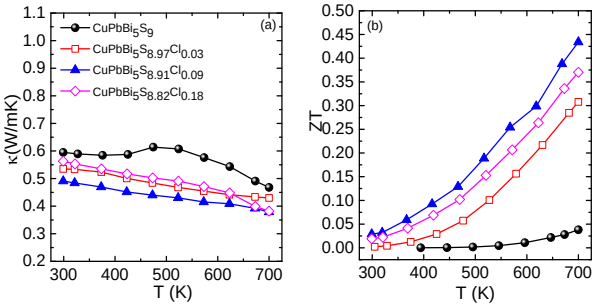

Fig. 1 (a) Total thermal conductivity and (b) thermoelectric figure of merit (ZT) of Cl-doped samples as a function of temperature.

References:
1. Liang, H., Guo, J., Zhou, Y., Wang, Z., Feng, Ge, Z. $CuPbBi_5S_9$ thermoelectric material with an intrinsic low thermal conductivity: Synthesis and properties. *Journal of Materiomics.* 2021, doi.org/10.1016/j.jmat.2021.03.016.
2. Kohatsu, I., Wuensch, B. J. The crystal structure of gladite, $PbCuBi_5S_9$, a superstructure intermediate in the series Bi_2S_3-$PbCuBiS_3$ (bismuthinite-aikinite). *Acta Crystallographica Section B.***1976** *32*, 2401-2409.

3. Petricek, V., Makovicky, E. Interpretation of selected structures of the bismuthinite - aikinite series as commensurately modulated structures Sample: supercell refinement. *The Canadian Mineralogist.* 2006, *44*, 189-206.

MOF-SILICON COMPOSITE FOR NEGATIVE LiB ELECTRODES FROM THEIR PREPARATION TO THEIR ELECTROCHEMICAL PERFORMANCES

Nassima KANA[1], Kaouther TOUIDJINE[1], Thomas DEVIC[1], Clémence SICARD[2], Bernard LESTRIEZ[1]

[1] *Université de Nantes, CNRS, Institut des Matériaux Jean Rouxel, IMN, F-44000 Nantes, France*

[2] *Université de Versailles St Quentin en Yvelines, CNRS, Institut Lavoisier, 78035 Versailles, France*

E-mail : nassima.kana@cnrs-imn.fr

Keywords: Metal organic frameworks; silicon anode; Li-ion battery; electrochemical performances

Silicon is considered as one of the most promising active materials for the anodes of Li-ion batteries with its high specific and volumetric capacities, about 3600 $mAh.g^{-1}$ and 2200 $mAh.cm^{-3}$ respectively[1]. However, during the lithiation (formation of Li_xSi, x ~ 3.75) the silicon undergoes an expansion of about 280% of its initial volume which induces numerous damages to the electrode: the silicon micrometer particles tend to be pulverized, the cohesion of the Si particles with each other and the adhesion of the Si electrode to the current collector are also damaged by these volume variations. This drastically reduces the electrochemical performance and lifetime of the Si electrode.[2] To circumvolve those issues, several studies have suggested to explore the properties of different Metal Organic Frameworks (MOFs) to improve the electrochemical performances of Si anode through coating layers on Si nanoparticles (NPs), which could act as an artificial solid electrolyte interface (SEI).[3,4,5] MOFs could be an efficient choice for several reasons: 1) the characteristics of the coordination bonds, notably their tunability, medium strength, and dynamic character, can confer to these materials original mechanical properties, which would be particularly adapted to the problem of the large and reversible volume variation of silicon electrodes;. 2) the porous nature of the MOF could facilitate the Li^+ diffusion contrary to other coatings. We focused our attention on the MOF A-520 or MIL-53(Al)-FA (FA =fumaric acid), with the formula $Al(OH)(fum)\cdot x\,H_2O$. This microporous solid (surface area ~ 1000 $m^2\ g^{-1}$) combine several advantages, such as its water-based synthesis at room pressure and temperature, non-toxic reactants (fumaric Acid and Al precursor) and a high yield production.[7] We explored various one-pot strategies to prepare MIL-53(Al)-FA coated silicon nanoparticles under mild conditions, compatible with standard procedures of preparation of silicon electrodes. Our goal is to achieve a uniform and thin MOF coating on the surface of Si NPs to perform it as an artificial SEI layer. We will here present the preparation and physico-chemical characterizations of these MOF-coated Si NPs (TGA, SEM, XRD and IR) as well as the electrochemical performances of the derived electrodes, which will be compared with the ones made of bare silicon.

1. Obrovac, M. N.; Chevrier, V. L. *Chem. Rev.* **2014**, *114* (23), 11444–11502.
2. Etiemble, A.; Tranchot, A.; Douillard, T.; Idrissi, H.; Maire, E.; Roué, L. *J. Electrochem. Soc.* **2016**, *163* (8), A1550–A1559.
3. Han, Y.; Qi, P.; Feng, X.; Li, S.; Fu, X.; Li, H.; Chen, Y.; Zhou, J.; Li, X.; Wang, B. *ACS Appl. Mater. Interfaces* **2015**, *7* (4), 2178–2182.
4. Malik, R.; Loveridge, Melanie. J.; Williams, L. J.; Huang, Q.; West, G.; Shearing, P. R.; Bhagat, R.; Walton, R. I. *Chem. Mater.* **2019**, *31* (11), 4156–4165.
5. Nazir, A.; Le, H. T. T.; Kasbe, A.; Park, C.-J. *Chem. Eng. J.* **2021**, *405*, 126963.
6. Devic, T.; Lestriez, B.; Roué, L. *ACS Energy Lett.* **2019**, *4* (2), 550–557.
7. Jeremias, F.; Fröhlich, D.; Janiak, C.; Henninger, S. K.. *RSC Adv* **2014**, *4* (46), 24073–24082.

ARTIFICIAL SEI FOR PROTON BATTERIES

Milad Toorabally,[1] Christel Laberty-Robert,[2] Damien Dambournet[3]

[1,2]*LCMCP,* [3]*PHENIX, Sorbonne Université, Paris, France*
Milad.toorabally@sorbonne-universite.fr, https://lcmcp.upmc.fr/site/

Keywords: Proton battery; HER; Layered titanate; Interlayer water

Summary:

Facing the growing need for energy demand, complementary solutions to Li-ion batteries are being studied. In our case, we are interested in a lamellar negative electrode material of TiO_2 capable of reversibly intercalating the proton. TiO_2, lepidocrocite type, organizes in sheets and has water in the inter-lamellar spaces. It is within this inter-lamellar that proton conduction by the Grotthus mechanism[1] will take place. To allow this initially insulating material to become conductive, different cations can be inserted during the hydrothermal synthesis, thus allowing the acceleration of the conduction of the proton[2]. This is what we will show with Zn^{2+} which has a positive impact on the electrochemical response of the material. Several levels of Zn^{2+} were tested: from 10 to 50 mol% relative to Ti^{4+}. The electrochemical properties of these materials (shaped with carbon black as conductive support and Nafion as binder) were studied in half-cell aqueous electrolyte buffered at pH 5 (CH_3COOH/CH_3COOK (1M)). Experimental capacities of more than 100 mAh/g and potentials up to -1.4V have been achieved, pushing back the phenomena of HER. The performance of these materials will be linked to their physicochemical characteristics, obtained by a panel of techniques adapted to amorphous materials.

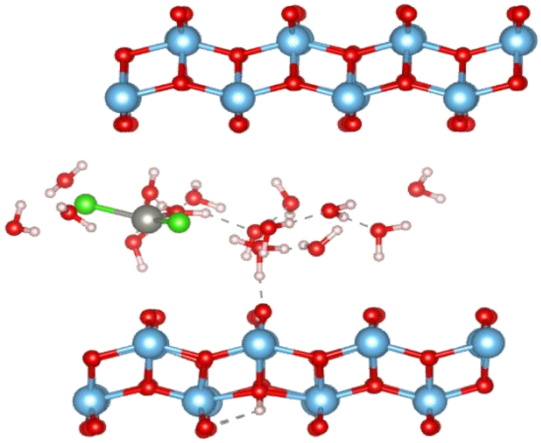

Fig. 1 Lepidocrocite type TiO2 with Zn^{2+} in the interlamellar space

References:
1. Wu, X.; Hong, J. J.; Shin, W.; Ma, L.; Liu, T.; Bi, X.; Yuan, Y.; Qi, Y.; Surta, T. W.; Huang, W.; Neuefeind, J.; Wu, T.; Greaney, P. A.; Lu, J.; Ji, X.. Nat. Energy 2019, 4 (2), 123–130
2. Kang,S; Singh.A; Badot,J-c; Reeves, K; Durand-vidal, Serge, Legein, C; Body, Monique, Dubrunfaut, O; Borkiewez, O; Tremblay, B; Laberty-Robert, C; Dambournet, D *Chemistry of Materials* **2020** *32* (21), 9458-9469

X-RAY MICRODIFFRACTION STUDY OF $LiMn_{1.5}Ni_{0.5}O_4$ THIN FILMS DEPOSITED BY SPUTTERING FOR LI-ION MICRO-BATTERIES APPLICATION

Clément LEVIEL[1,2,4], Ankush BHATIA[3], Maxime HALLOT[2,4], Florent BLANCHARD[1], Jean-Pierre PEIREIRA RAMOS[3], Rita BADDOUR-HADJEAN[3], Christophe LETHIEN[2,4], Pascal ROUSSEL[1]

[1]*Unité de Catalyse et de Chimie du Solide, Université de Lille, CNRS, UMR 8181 – UCCS, Lille, France*
[2]*Institut d'Électronique, de Microélectronique et de Nanotechnologies, Université de Lille, CNRS, UMR 8520 - IEMN, Lille, France*
[3]*Institut de Chimie et des Matériaux Paris-Est, Université Paris-Est Créteil, CNRS, UMR 7182 – ICMPE, Thiais, France*
[4]*Réseau sur le Stockage Electrochimique de l'Energie (RS2E), CNRS FR 3459, Amiens, France*
clement.leviel.etu@univ-lille.fr, https://uccs.univ-lille.fr/

$LiMn_{1.5}Ni_{0.5}O_4$, Micro-battery, X-ray micro-diffraction, Magnetron sputtering, thin film

The emergence of new miniaturized and autonomous electronic technology results in demand for small electrochemical energy storage devices. The development of high performance Li-ion micro batteries with thick sputtered films is an attractive way to increase considerably the performance while keeping a low surface footprint.
We are currently working on a promising spinel type electrode material, $LiMn_{1.5}Ni_{0.5}O_4$ (LMNO), made from magnetron sputtering deposition method (thin film) on Si/Al_2O_3/Pt substrate [1].
LMNO is a high working potential electrode (E_{Li/Li^+} = 4.8V vs Li/Li^+) with a good experimental discharge capacity (60µAh cm^{-2} $µm^{-1}$) really close to the theoretical value (65µAh cm^{-2} $µm^{-1}$) and is able to sustain high rate cycling. However, the electrochemical properties are closely related to various parameters such as the crystal orientation, Ni and Mn cation ordering (ordered or disordered spinel) [2] and thickness of the films. In order to improve the performance of Li-ion micro-batteries, it is crucial to understand the different mechanisms involved, but also their evolution during the different cycles of charge/discharge. It is therefore important to tune the characterization techniques allowing the analysis of the structural evolution of micro-batteries active materials such as X-ray diffraction (XRD), X-ray absorption spectroscopy (XAS) or transmission electron microscopy (TEM). If it is relatively common to follow in situ / operando bulk material for large scale Li-ion batteries, adapting these techniques to their miniaturized counterparts (i.e. the micro-batteries) is challenging as highlighted in the article published by Qu, Z & al. in 2020 [3]. However, we have shown that the XAS synchrotron operando study of vanadium nitride thin films used as electrode materials for micro supercapacitors could give valuable insights on the storage mechanism [4].
We thus decided to study this material by X-ray micro-diffraction on a Rigaku SmartLab with 9 kW rotating anode X-ray source. This technique allows performing XRD patterns on 400 microns area [5].
We use this technique for mapping our thin films to verify their homogeneity, perform ex-situ analyses at different state of electrode charge or after different number of charge/discharge cycles. We also link our XRD studies with other complementary characterization techniques to obtain a global view of the characteristics of our thin films. For example, Figure 1, I shows the integrated intensity of the (400) and (440) diffraction peak from a micro-XRD mapping study of a 1-micron thick wafer of LMNO. The figure 1, II shows the X-ray micro-fluorescence study of the same wafer with the analysis of the manganese nickel ratio according to the position on the wafer.

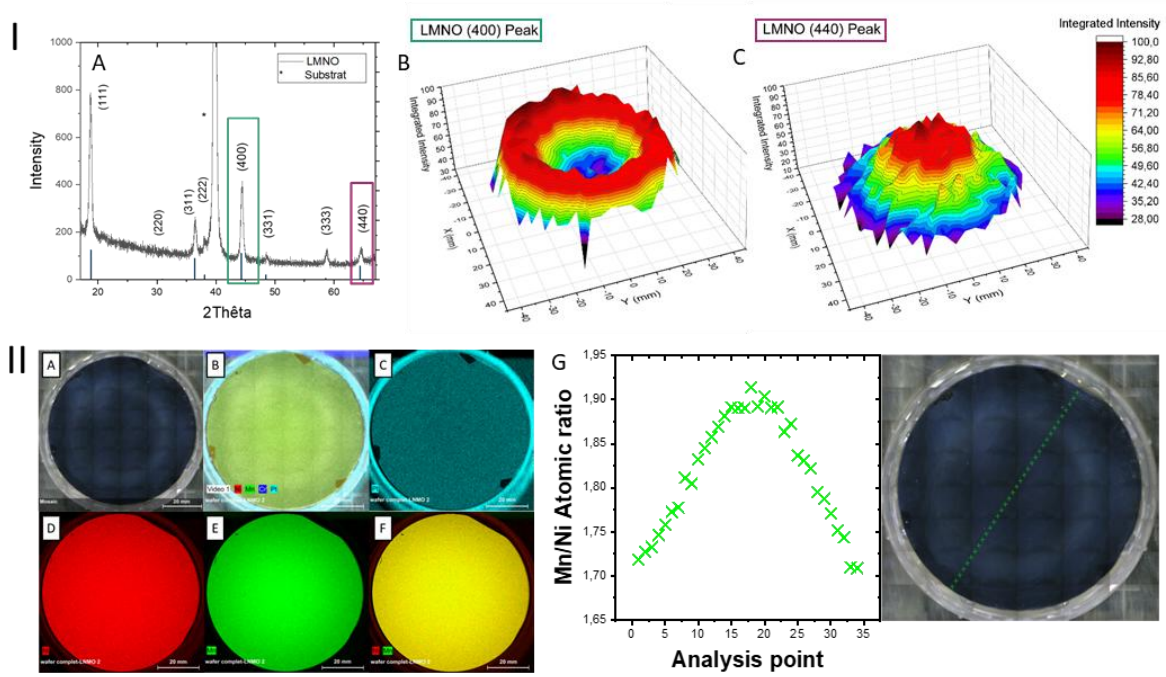

Fig. 1 **I**,**A** LMNO wafer mapping of the (400) **B** and (440) **C** diffraction peaks. **II** Elemental mapping of a LMNO wafer **A** by micro-fluoX of platinum **C**, nickel **D** and manganese **E** and analysis of the manganese nickel ratio according to the position on the wafer **G**.

References:

1. M. Hallot & al. Sputtered LiMn1.5Ni0.5O4 Thin Films for Li-Ion Micro-Batteries with High Energy and Rate Capabilities. Energy Storage Mater. **2018,** 15, 396–406.

2. Julien, C. M. et al. Comparative Issues of Cathode Materials for Li-Ion Batteries. Inorganics. **2014**, 2 (1), 132–154.

3. Qu, Z. et al. Towards High-Performance Microscale Batteries: Configurations and Optimization of Electrode Materials by in-Situ Analytical Platforms. Energy Storage Mater. **2020**, 29, 17–41.

4. K. Robert et al. Novel insights into the charge storage mechanism in pseudocapacitive vanadium nitride thick films for high-performance on-chip microsupercapacitors. Energy Environ. Sci. **2020**, 13, 949.

5. M. Hallot & al. Atomic Layer Deposition of a Nanometer-Thick Li3PO4 Protective Layer on LiNi0.5Mn1.5O4 Films: Dream or Reality for Long-Term Cycling? ACS Appl. Mater. Interfaces. **2021**, 13, 15761–15773.

NEW LITHIUM RICH LAYERED OXIDES AS POSITIVE ELECTRODE MATERIALS FOR LI-ION BATTERY APPLICATION

Valentin SAIBI,[1] Laurent CASTRO,[2] Claude DELMAS,[1] Marie GUIGNARD [1]

[1] *ICMCB-CNRS, Pessac, France*
[2] *Toyota Motor Europe, Zaventem, Belgium*
valentin.saibi@icmcb.cnrs.fr, www.icmcb-bordeaux.cnrs.fr

Keywords: layered oxides, O2-type structure, ion-exchange reaction, powder diffraction, stacking faults, Li-ion battery

Summary:
O3-type lithium-rich layered oxides with the general formula $Li_{1+x}M_{1-x}O_2$ (M = transition metal cations) have been intensively studied as positive electrode materials in Li-ion batteries due to their high lithium (de)intercalation rate, providing high specific capacity (>225mAh/g with $Li_{1.2}Ni_{0.13}Co_{0.13}Mn_{0.54}O_2$) thanks to additional anionic oxygen redox at high voltage [1]. However, their practical application is partly hindered by continuous capacity loss and voltage fading after the first cycle, primarily due to the irreversible migration of manganese ions within the lithium layers leading to the formation of a spinel-like structure at the surface of the particles [2].
To overcome this problem, we decided to synthetize new cobalt-free lithium-rich layered oxides with an O2-type structure (**Fig.1**). This particular oxygen stacking with alternative of face- and edge-sharing LiO_6 and MO_6 octahedra would make the migration of manganese ions more reversible thanks to stronger coulombic repulsions between the layers. Batteries made with this material show high specific capacity with an improved reversibility over twenty cycles [3]. However, O2-phases are metastable and cannot be obtained directly. For that reason, a P2-type sodium layered oxide is used as a precursor for an ion-exchange reaction towards the desired O2-type lithium-rich layered oxide.
The Na^+-to-Li^+ ion-exchange reaction is associated with gliding of transition metal layers. These translations are presumably not collaborative and result in stacking faults in the material [4]. In order to better understand the structure of this ion-exchanged O2-type lithium-rich layered oxide, X-ray diffraction patterns have been simulated with *Faults*. Their comparison with the experimental synchrotron X-ray diffraction pattern confirms the existence of defaults in the oxygen stacking along the *c* axis where a specific environment for lithium ions in the interslab tends to be favored.

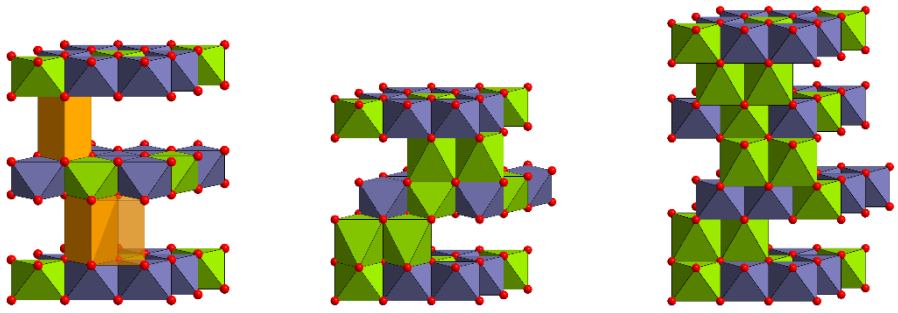

Fig.1 *(a) P2-, (b) O2- and (c) O3-type structures in $A_{1+x}M_{1-x}O_2$ layered oxides with NaO_6 prism (orange), LiO_6 octahedra (green) and MO_6 octahedra (purple)*

References:
[1] H. Koga, L. Croguennec, P. Mannessiez, M. Ménétrier, F. Weill, L. Bourgeois, M. Duttine, E. Suard, C. Delmas, *J. Phys. Chem. C* **2012**, *116*, 13497.
[2] D. Eum, B. Kim, S. J. Kim, H. Park, J. Wu, S.-P. Cho, G. Yoon, M. H. Lee, S.-K. Jung, W. Yang, W. M. Seong, K. Ku, O. Tamwattana, S. K. Park, I. Hwang, K. Kang, *Nat. Mater.* **2020**, *19*, 419.
[3] B. M. de Boisse, J. Jang, M. Okubo, A. Yamada, *J. Electrochem. Soc.* **2018**, *165*, A3630.
[4] N. Yabuuchi, R. Hara, M. Kajiyama, K. Kubota, T. Ishigaki, A. Hoshikawa, S. Komaba, *Adv. Energy Mater.* **2014**, *4*, 1301453.